Highlights on top quark physics with the ATLAS experiment at the LHC

PIC2024 - The 43rd International Symposium on Physics in Collision, Athens

Emily Hampshire (Royal Holloway, University of London)

Top-quark physics at the ATLAS experiment

- Top quark decays before hadronization and **information about its spin state is preserved** in the distributions of its decay products.
- Top quark mass is key ingredient **in EW precision and QCD calculations**.
- Top quark couplings to SM bosons and top quark decay products are **sensitive to BSM particles**.
- Broad program of top-quark physics at the ATLAS experiment.
- Will focus on five recent results:
  - Search for same-charge top-quark pair production in pp collisions at $\sqrt{s} = 13$ TeV (arXiv:2409.14982)
  - Measurement of top-quark pair production in association with charm quarks in proton-proton collisions at $\sqrt{s} = 13$ TeV (arXiv:2409.11305)
  - Measurement of $t\bar{t}$ production in association with additional b-jets in the $e\mu$ final state in proton-proton collisions at $\sqrt{s} = 13$ TeV (arXiv:2407.13473)
  - Test of lepton flavour universality in W-boson decays into muons and electrons in pp collisions at $\sqrt{s} = 13$ TeV (arXiv:2403.02133)
  - Observation of $t\bar{t}$ production in the lepton+jets and dilepton channels in p+Pb collisions at $\sqrt{s_{NN}} = 8.16$ TeV (arXiv:2405.05078)

arXiv:2409.14982

Search for same-charge top-quark pair production in pp collisions at $\sqrt{s}$= 13 TeV with the ATLAS detector

ATLAS EXPERIMENT

1

[arXiv:2409.14982]

Same-charge top-quark pair production

- Same-charge (same-sign, SS) top pair production (tt or $\bar{t}\bar{t}$) is **strongly suppressed in the SM**
  - SS top-quark pair production is forbidden at LO in perturbation theory
- First ATLAS search for SS top-quark pairs using **SMEFT with pointlike four-fermion interactions**
- Three four-fermion operators are considered:
  - $O_{tu}^{(1)}, O_{Qu}^{(1)}, O_{Qu}^{(8)}$ with Wilson Coefficients (WCs) $c_{tu}^{(1)} = 0.04$, $c_{Qu}^{(1)} = 0.1$, $c_{Qu}^{(8)} = 0.2$ and new physics energy scale $\Lambda = 1$ TeV
  - Corresponds to cross-sections $\sigma(pp \to tt) = 97.6$ fb and $\sigma(pp \to \bar{t}\bar{t}) = 2.4$ fb → **highly charge asymmetric.** Different WCs setups by **reweighting**.

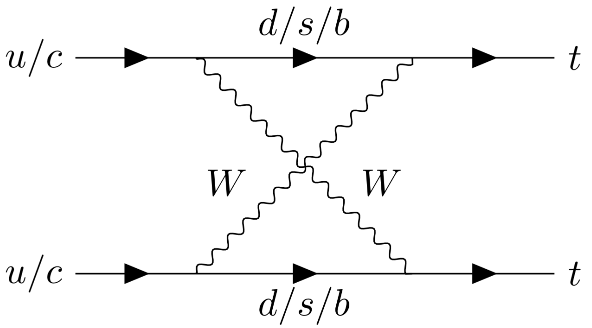

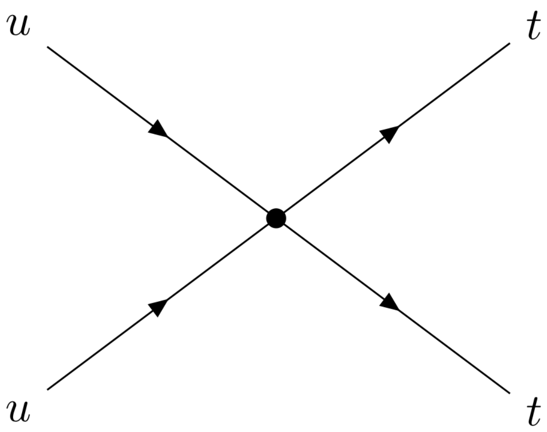

arXiv:2409.14982

Same-charge top-quark pair production

- Analysis Strategy:
  - Selection: 2 same-charge (SC) leptons, 2 b-jets, missing transverse momentum
  - Full Run 2 pp collisions at $\sqrt{s} = 13$ TeV with 140 $\mathbf{fb}^{-1}$
  - Neural network, NN^{SvsS}, used to discriminate signal events originating from $c_{tu}^{(1)}$ vs $c_{Qu}^{(1)}$ or $c_{Qu}^{(8)}$
  - These are split by lepton charge, ++ or - -, due to different kinematics for tt and $\overline{tt}$, and NN^{SvsB} **are trained to separate signal and background**
  - Signal regions (SRs) additionally required $\Delta\phi_{l,l} \geq 2.5$ and validation region (VRs) $\Delta\phi_{l,l} < 2.5$ to validate the background modelling.
  - Control regions (CRs) used to constrain normalisation of major background processes. **Binned profile likelihood fits over SRs and CRs simultaneously**.

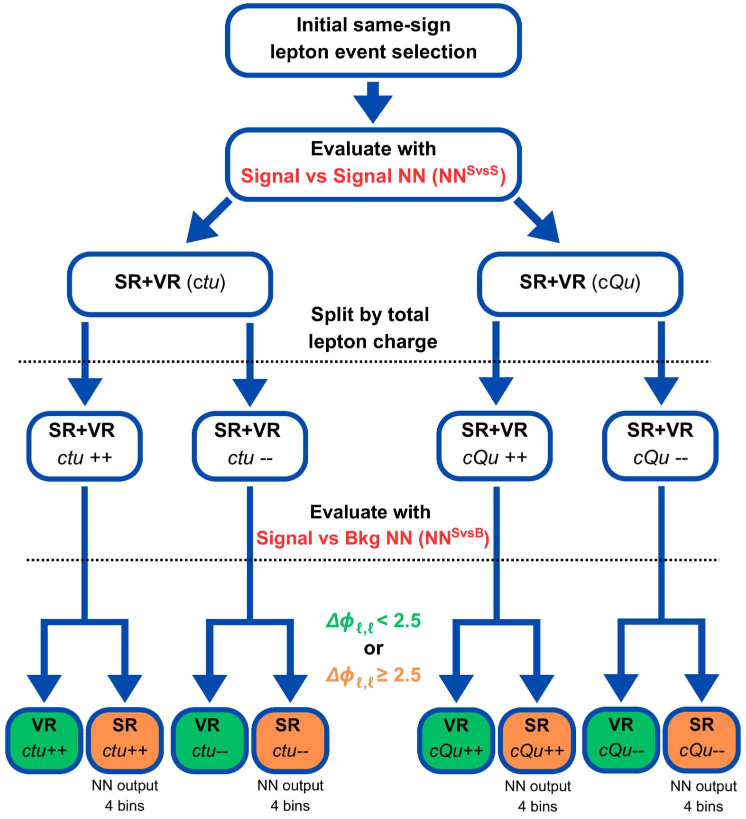

arXiv:2409.14982

Same-charge top-quark pair production

- **Statistically-limited results**, largest systematic uncertainty from $t\bar{t}W$ modelling uncertainties.
- Largest background from $t\bar{t}W$ events.
- Good post-fit agreement in CRs and SRs. **Results are in agreement with SM**
- Observed (expected) upper limit on production cross-section at 95% CL:

  $\sigma(pp \to tt) < 1.6\ (2.0)$ fb
- 1D limits set on WCs by varying single WC at a time, the observed (expected) limits at 95% CL: $c_{tu}^{(1)} < 0.0068\ (0.0071)$, $c_{Qu}^{(1)} < 0.020\ (0.022)$, $c_{Qu}^{(8)} < 0.041 (0.046)$
- These are **most stringent limits on WCs, improving previous limits by factor ≈ 10**

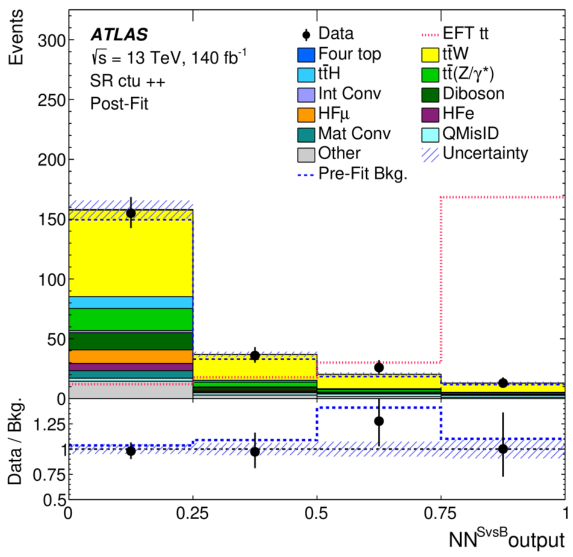

Uncertainties	Wilson Coefficient CIs at 95% CL ($\times 10^{-2}$)		
	$c_{tu}^{(1)}$	$c_{Qu}^{(1)}$	$c_{Qu}^{(8)}$
Statistical uncertainty only	[-0.65, 0.65]	[-1.9, 1.9]	[-3.9, 3.9]
Statistical + modeling uncertainties	[-0.67, 0.67]	[-1.9, 1.9]	[-4.0, 4.0]
Total uncertainty	[-0.68, 0.68]	[-2.0, 2.0]	[-4.1, 4.1]

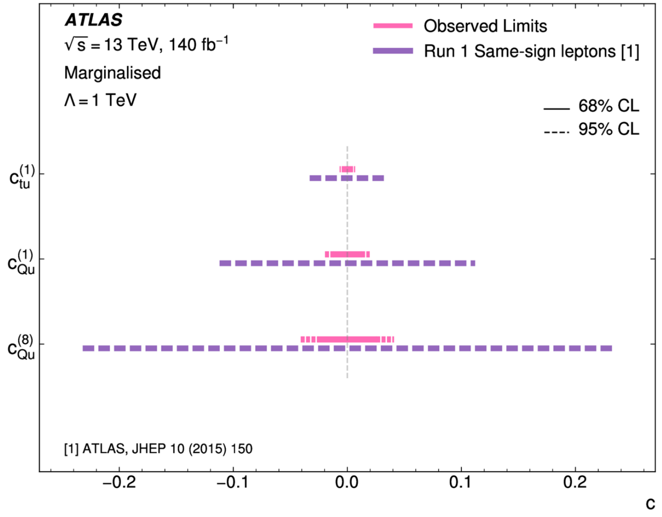

arXiv:2409.11305

Measurement of top-quark pair production in association with charm quarks in proton–proton collisions at $\sqrt{s}$= 13 TeV with the ATLAS detector

ATLAS EXPERIMENT

2

Inclusive cross-section $t\bar{t}$ + charm jets

- $t\bar{t}$ + heavy-flavour (HF) jets (c-jets, b-jets) is **large irreducible background** to many analyses (e.g. $t\bar{t}H$ with $H \rightarrow b\bar{b}$)
- $t\bar{t}$ + HF is **challenging to model** due to scale hierarchy from $t\bar{t}$ production to $b\bar{b}/c\bar{c}$ production from gluon emission.
- Analysis strategy:
  - Single lepton (1L) and dilepton (2L) final states, (e, μ)
  - Simultaneous identification of b-jets and c-jets – utilises **custom b/c flavour-tagging algorithm** with the WPs:
    - c@11%, c@22% (with b-jet rejection rates 28.7 and 18.9),
    - b@60%, b@70% (with c-jet rejection rates 37.1 and 12.2)
  - Fit in 19 regions (12 control regions, 4 1L signal regions, 3 2L signal regions) using profile likelihood fit
    - POIs: $t\bar{t} +\geq 2c$ and $t\bar{t} + 1c$ signal strengths
    - Normalisation factors for $t\bar{t} +\geq 1b$ and $t\bar{t}$ + light are free-floating
  - Measure cross-sections in fiducial phase space and cross-section ratios in more inclusive phase space

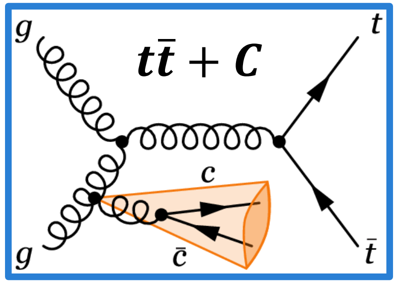

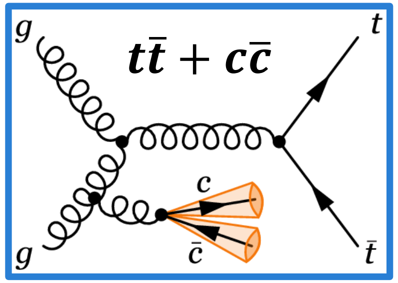

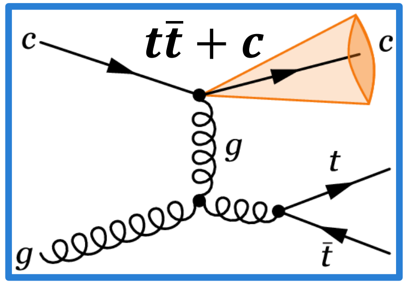

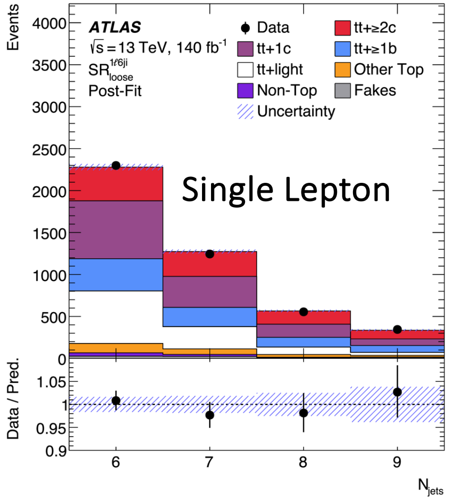

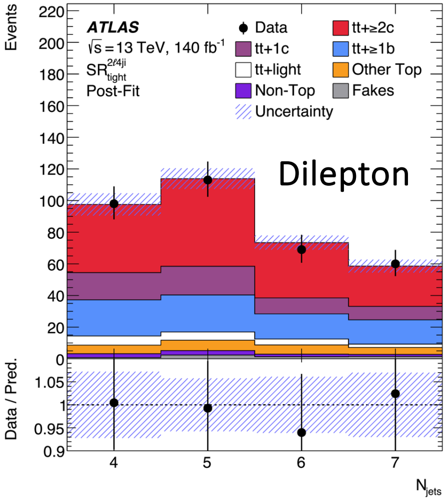

Inclusive cross-section $t\bar{t}$ + charm jets

- Fiducial cross-sections

$$\sigma^{\text{fid}}(t\bar{t} + \geq 2c) = 1.28^{+0.16}_{-0.10}(\text{stat})^{\pm 0.21}_{-0.22}(\text{syst})\ \text{pb}$$
$$= 1.28^{+0.27}_{-0.24}\ \text{pb}$$
$$\sigma^{\text{fid}}(t\bar{t} + 1c) = 6.4^{+0.5}_{-0.4}(\text{stat}) \pm 0.8\ (\text{syst})\ \text{pb}$$
$$= 6.4^{+1.0}_{-0.9}\ \text{pb}$$

- **Largest uncertainties from $t\bar{t} + \geq 1c$ signal modelling, calibration of b/c-tagger, and data statistics.**
- NLO+PS predictions for $t\bar{t} + \geq 2c$ and $t\bar{t} + 1c$ cross-sections are **largely consistent with measured results** but **underpredict by 0.5 to 2.0 standard deviations.**
- Measured cross-section ratios of $t\bar{t} + \geq 2c$ and $t\bar{t} + 1c$ to total $t\bar{t}$ + jets production in more inclusive phase space as:

$$R^{\text{inc}}_{t\bar{t}+\geq 2c} = (1.23 \pm 0.25)\% \text{ and } R^{\text{inc}}_{t\bar{t}+1c} = (8.8 \pm 1.3)\%$$

- These are **in agreement with POWHEG+PYTHIA8 simulations** within 0.9 and 1.1 standard deviations.

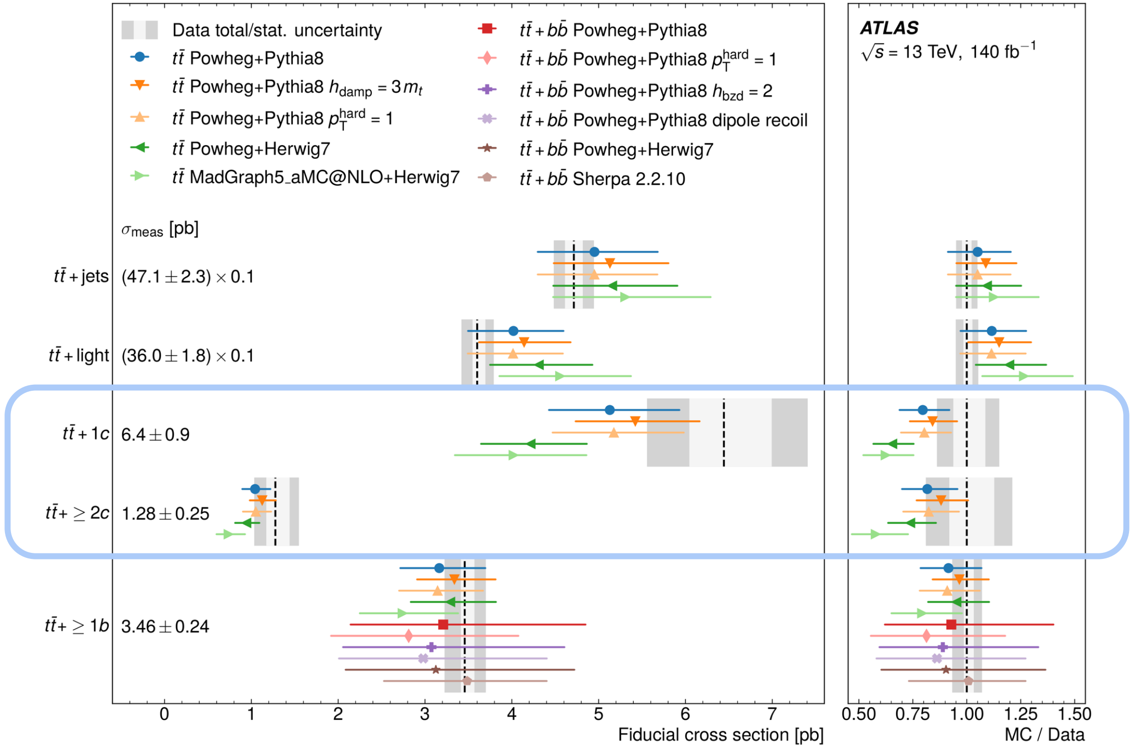

arXiv:2407.13473

Measurement of $t\bar{t}$ production in association with additional b-jets in the $e\mu$ final state in proton–proton collisions at $\sqrt{s}$ = 13 TeV with the ATLAS detector

3

ATLAS EXPERIMENT

arXiv:2407.13473

$t\bar{t}$+ b-jets production in $e\mu$ final state

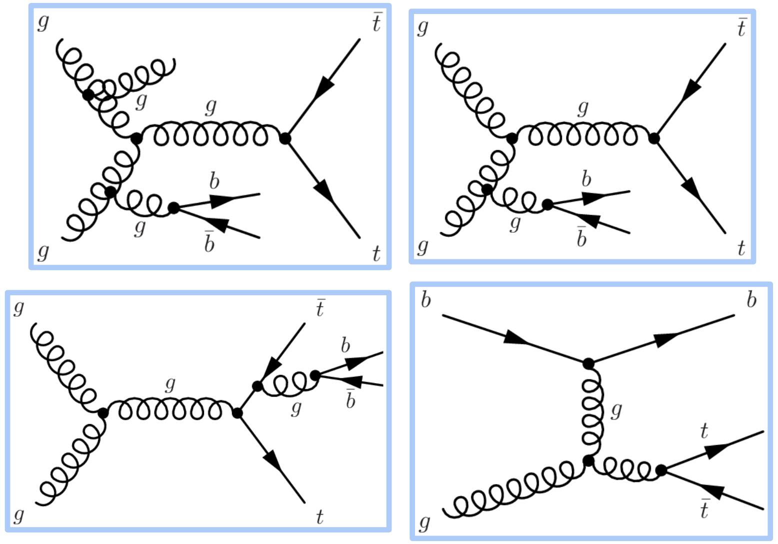

- Analysis strategy:
  - Select OS $e\mu$, ≥ 2 jets, ≥ 2 b-jets (DL1r 77% efficiency)
  - **Fiducial integrated cross-sections** in 4 regions: $e\mu +$ $\geq 3b \mid \geq 4b \mid \geq 3b + \geq 1l/c \mid \geq 4b + \geq 1l/c$
  - **Normalised fiducial differential cross-sections**
  - After subtracting the estimated background, the data is **unfolded to particle-level** using an iterative Bayesian technique
- A kinematic algorithm is developed for the classification of the origin of b-jets (from $t\bar{t}$ or gluon radiation). **The probability of correct assignment of a b-jet (≥2 b-jets), in a given bin, ranges from 50% to 85% (40% to 75%).**
- Significant **background from mistagged jets in $t\bar{t}$+light and $t\bar{t}$+c events**.
  - To **reduce the impact of systematic uncertainties** in these backgrounds → template fits to data are performed to extract normalisation factors for $t\bar{t}$+b, $t\bar{t}$+light and $t\bar{t}$+c at particle-level.
  - The data are found to be **described much better by the predictions after the individual $t\bar{t}j$ components are corrected**.

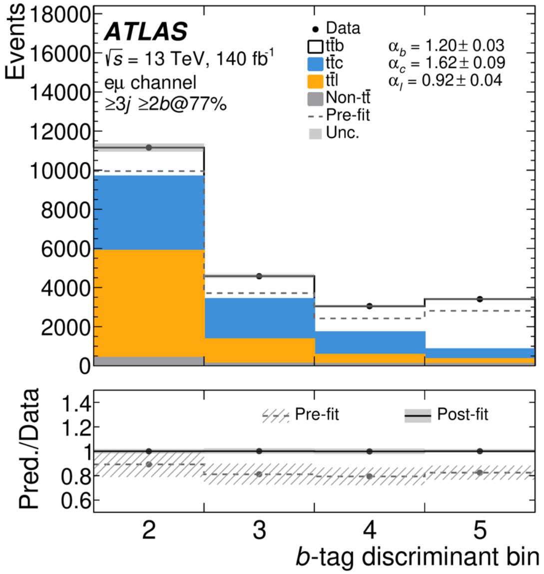

arXiv:2407.13473

$t\bar{t}$+ b-jets production in $e\mu$ final state

- Fiducial cross-section results **are dominated by systematic uncertainties**, primarily from b-tagging, jet energy scale, and $t\bar{t}$ modelling.
- The precision of these results **surpasses previous results using partial 13 TeV ATLAS data**.
- Differential cross-section results **show good agreement** with predictions for most observables in a quantitative comparison.

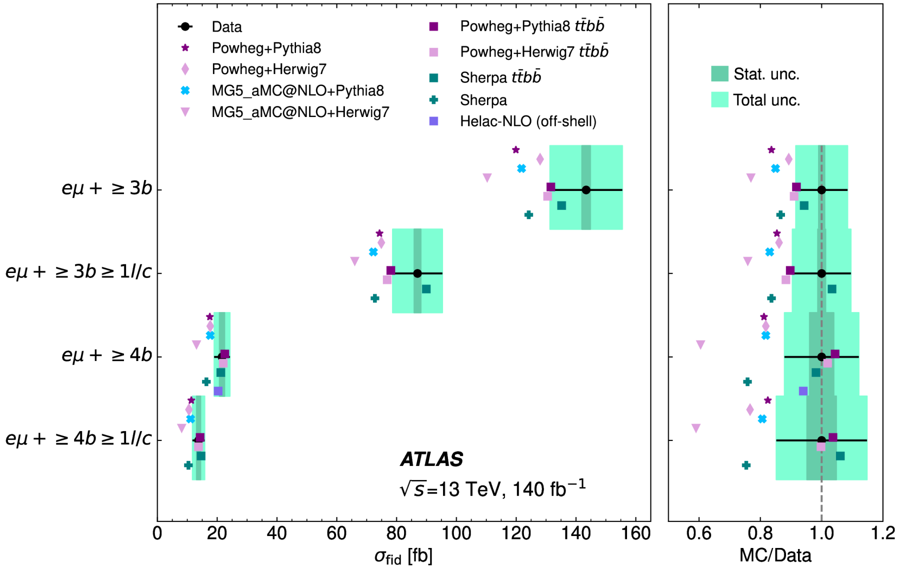

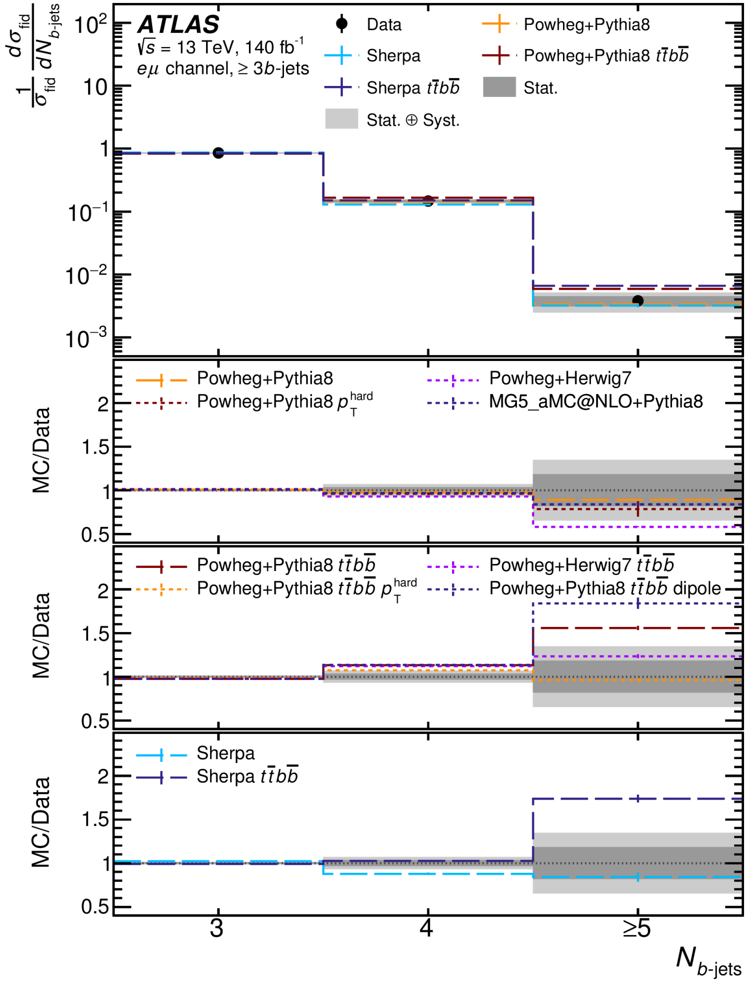

arXiv:2403.02133

Precise test of lepton flavour universality in W-boson decays into muons and electrons in pp collisions at $\sqrt{s}$ = 13TeV with the ATLAS detector

ATLAS EXPERIMENT

4

arXiv:2403.02133

LFU in W-boson decays to e, μ

- Lepton Flavour Universality (LFU) is fundamental axiom of SM:
  - Couplings of charged leptons to EW gauge bosons are **independent** of the lepton flavour
- Flavour anomalies in b-hadron decays hint at **departures from LFU**
- Analysis strategy:
  - Select $t\bar{t}$ events with OS ee | $e\mu$ | $\mu\mu$ and 1 or 2 b-jets
  - Measure ratio (normalised using LEP+SLD measurement of $Z \rightarrow ll$ events to reduce lepton identification uncertainties):

$$R_{WZ}^{\mu/e} = \frac{R_W^{\mu/e}}{\sqrt{R_Z^{\mu\mu/ee}}} = \frac{\mathcal{B}(W\rightarrow\mu\nu)}{\mathcal{B}(W\rightarrow e\nu)} \cdot \sqrt{\frac{\mathcal{B}(Z\rightarrow ee)}{\mathcal{B}(Z\rightarrow\mu\mu)}}$$

- Muon reweighting in p_T and η to reduce kinematic differences between e and μ, to **minimise physics modelling uncertainties**.
- Measurement of lepton isolation efficiencies – for $t\bar{t} \rightarrow ll$ and $Z \rightarrow ll$ events and compared to POWHEG+PYTHIA8 and SHERPA simulation samples

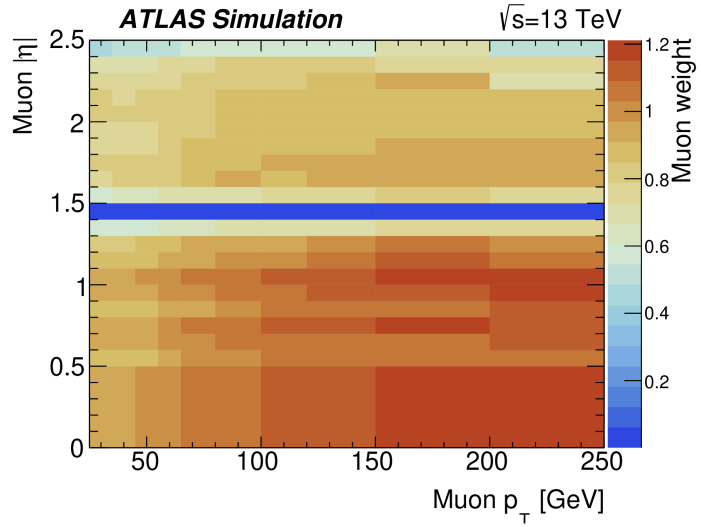

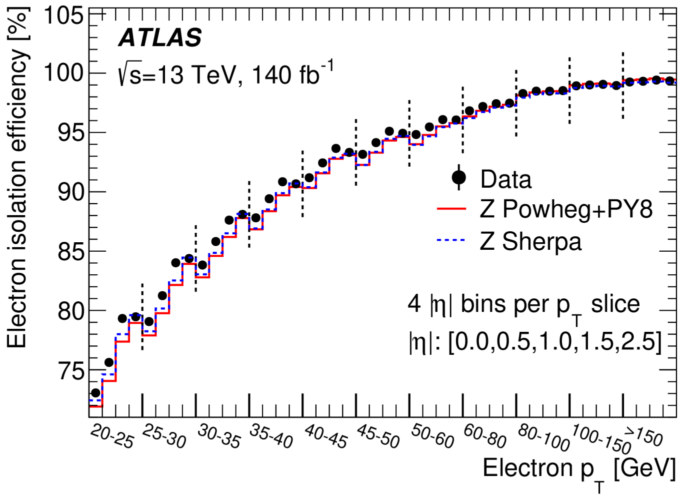

arXiv:2403.02133

LFU in W-boson decays to e, μ

- Simultaneous **maximum likelihood fit** to $t\bar{t}$ events and $Z \rightarrow ll$ counts with four POIs: $\sigma_{t\bar{t}}, \sigma_{Z\rightarrow ll}, R_{WZ}^{\mu/e}, R_{Z}^{\mu\mu/ee}$
- Yields for $t\bar{t} \rightarrow e\mu$ and $Z \rightarrow ll$ regions, m_{ll} spectrum for $t\bar{t} \rightarrow ee, \mu\mu$ regions.
- The ratios were fitted to be:

$$R_{WZ}^{\mu/e} = 0.9990 \pm 0.0022(\text{stat}) \pm 0.0036(\text{syst})$$

$$R_{Z}^{\mu\mu/ee} = 0.9913 \pm 0.0002(\text{stat}) \pm 0.0045(\text{syst})$$

$$R_{WZ}^{\mu/e} = \frac{R_W^{\mu/e}}{\sqrt{R_Z^{\mu\mu/ee}}} = \frac{\mathcal{B}(W \rightarrow \mu\nu)}{\mathcal{B}(W \rightarrow e\nu)} \cdot \sqrt{\frac{\mathcal{B}(Z \rightarrow ee)}{\mathcal{B}(Z \rightarrow \mu\mu)}}$$

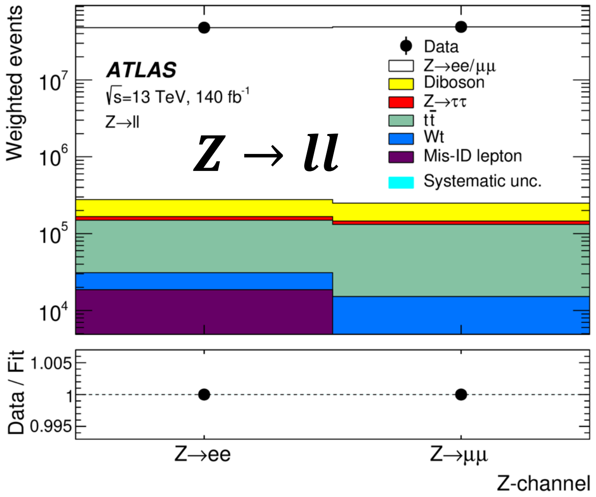

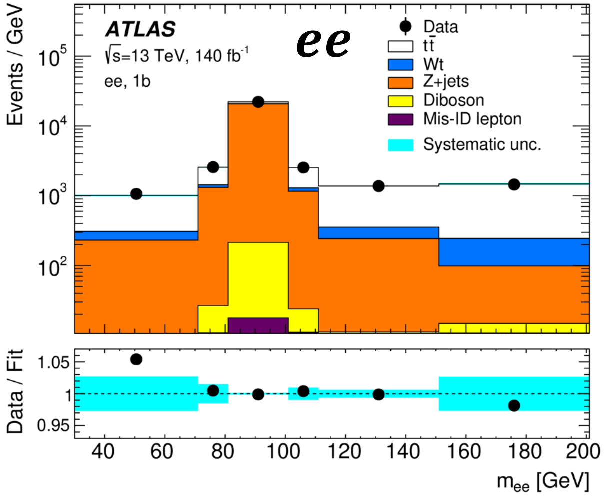

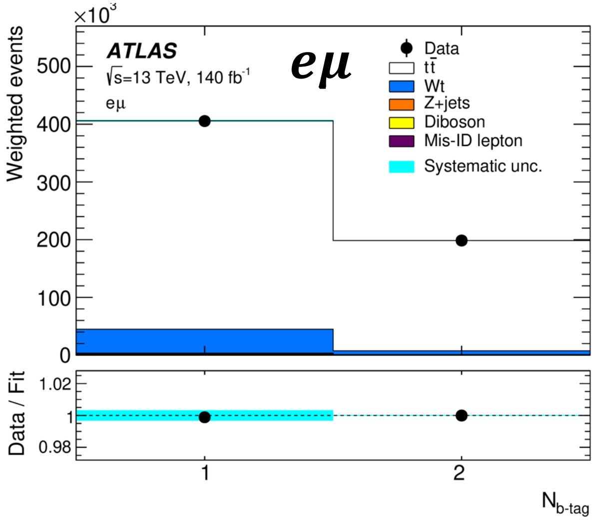

arXiv:2403.02133

LFU in W-boson decays to e, μ

- The external LEP+SLD measurement of

$$R_{Z-\mathrm{ext}}^{\mu\mu/ee} = 1.0009 \pm 0.0028$$

- was used to calculate

$$R_W^{\mu/e} = 0.9995 \pm 0.0022(\mathrm{stat}) \pm 0.0036(\mathrm{syst}) \pm 0.0014(\mathrm{ext})$$
$$= 0.9995 \pm 0.0045$$
$$= \frac{\mathcal{B}(W\to\mu\nu)}{\mathcal{B}(W\to e\nu)}$$

- **Dominated by systematic uncertainties**: PDF, modelling, lepton uncertainties
- **Consistent with lepton flavour universality** and with previous measurements
- **Higher precision than previous world average**

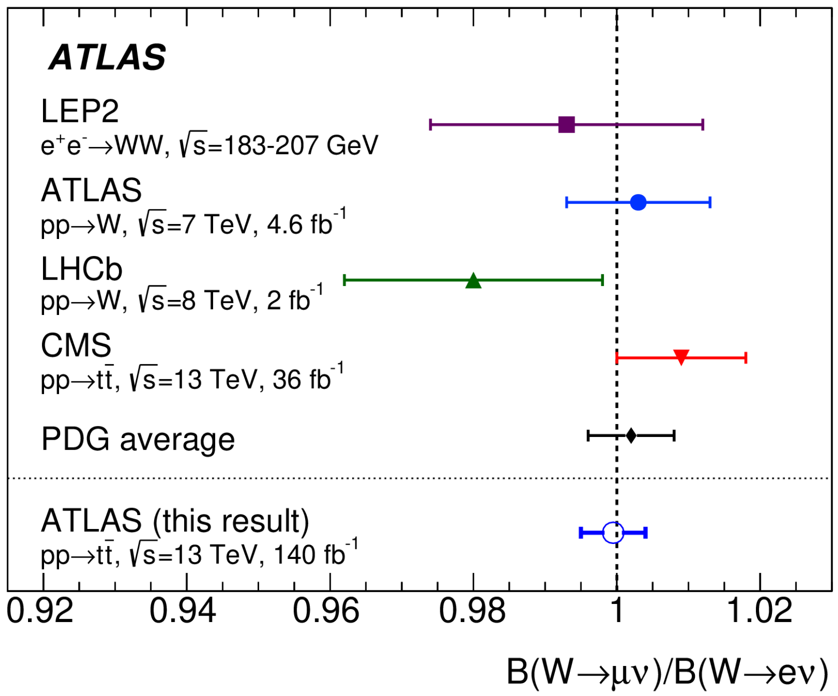

arXiv:2405.05078

Observation of $t\bar{t}$ production in the lepton+jets and dilepton channels in p+Pb collisions at $\sqrt{s_{NN}}$ = 8.16 TeV with the ATLAS detector

ATLAS EXPERIMENT

5

[arXiv:2405.05078](https://arxiv.org/abs/2405.05078)

$t\bar{t}$ production in p+Pb collisions

- Strongly interacting **quark-gluon plasma (QGP)** in Pb-Pb collisions
- Pb+Pb collisions differ from pp collisions due to **initial-state effects** (parton distribution functions (PDFs)) and **final-state effects** (creation of QGP)
- Gain knowledge of initial state effects using **p+Pb collisions**
- Use top quarks to **probe nuclear PDFs (nPDFs)** in kinematic region of Bjorken-$x \sim 5 \cdot 10^{-3} - 0.05$ and $Q^2 \sim m_t^2 \sim 3 \cdot 10^4$ GeV^2
- Analysis strategy:
  - 165 nb^{-1} of p+Pb data at $\sqrt{s_{NN}} = 8.16$ TeV in 2016
  - Define two channels: $1l, \geq 4j, \geq 1$ b-jet | $2l, \geq 2j, \geq 1$ b-jet ($l = e, \mu$)
  - Split into 2 dilepton SRs and 4 lepton+jets SRs
  - **Binned profile likelihood fit** with POI: $\mu_{t\bar{t}}$ = ratio of observed signal over SM expectation with no nPDF effects.
  - Dilepton channel background **dominated by Z+jets and single top tW events**. Lepton+jets has largest background contributions from **W+jets and fake leptons**.

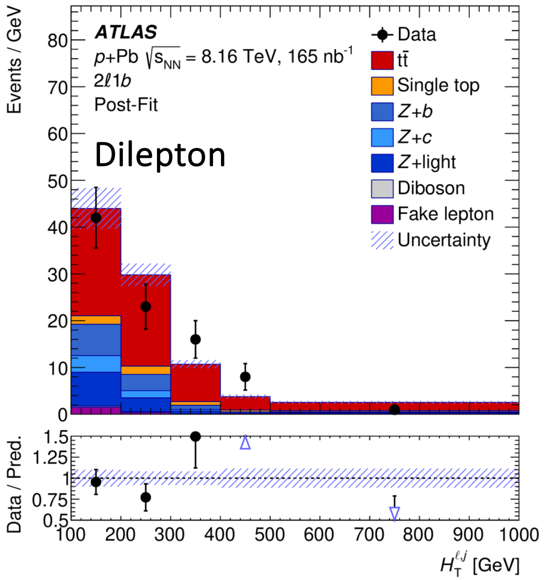

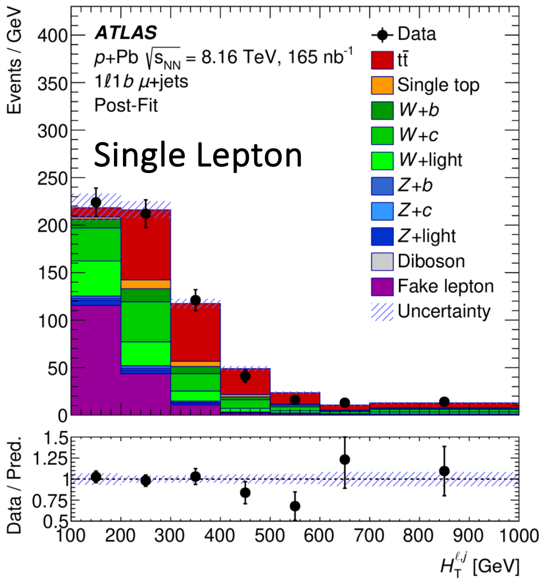

arXiv:2405.05078

$t\bar{t}$ production in p+Pb collisions

- **Limited by systematic uncertainties in lepton+jets** SRs and by **statistical uncertainties in dilepton** SRs.
- Largest sources of systematic uncertainties from **jet energy scale and signal modelling**.
- Background-only hypothesis is rejected with a significance of more than 5 standard deviations – **observation of $t\bar{t}$ process in p+Pb collisions by ATLAS**
- The inclusive $t\bar{t}$ cross-section is measured:

$$\sigma_{t\bar{t}} = 58.1 \pm 2.0(\text{stat})^{+4.8}_{-4.4}(\text{syst})\ \text{nb} = 58.1^{+5.2}_{-4.9}\ (\text{tot})\ \text{nb}$$

- **Most precise $t\bar{t}$ cross-section measured in nuclear collisions to date**
- In agreement with CMS result within 1.4 standard deviations.

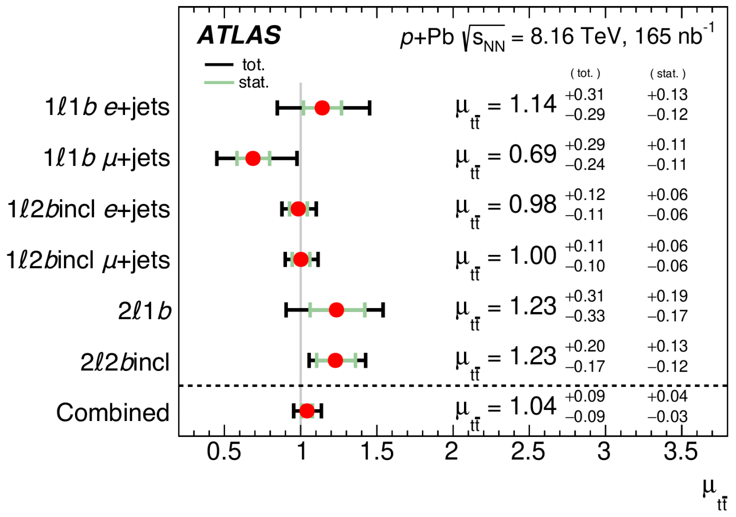

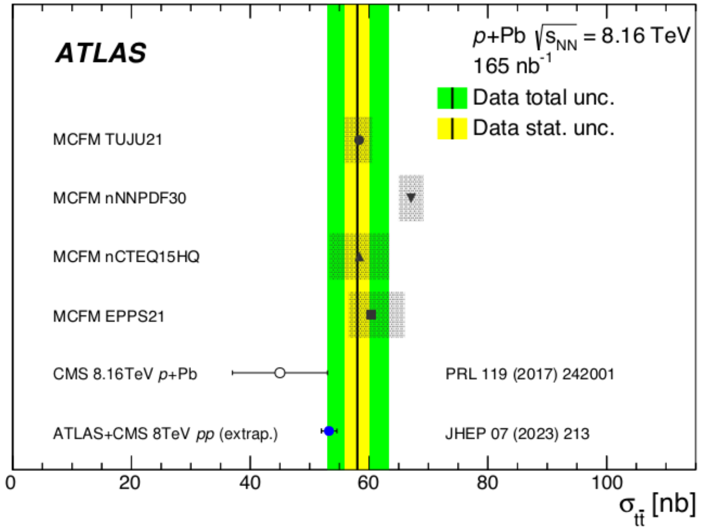

arXiv:2405.05078

$t\bar{t}$ production in p+Pb collisions

- Additionally, measured the **nuclear modification factor**, for the first time at LHC.
- Using measured $t\bar{t}$ cross-section in pp collisions at $\sqrt{s} = 8$ TeV, $\sigma_{t\bar{t}}^{pp}$, and mass number of Pb nucleus, A_{Pb}=208, this is defined as:

$$R_{pA} = \frac{\sigma_{t\bar{t}}^{p+Pb}}{A_{Pb} \cdot \sigma_{t\bar{t}}^{pp}}$$

$$= 1.090 \pm 0.039(\text{stat})^{+0.094}_{-0.087}(\text{syst}) = 1.090 \pm 0.100(\text{tot})$$

- Systematics-limited
- **Consistent with unity within uncertainties** and **good agreement with predicted values**.

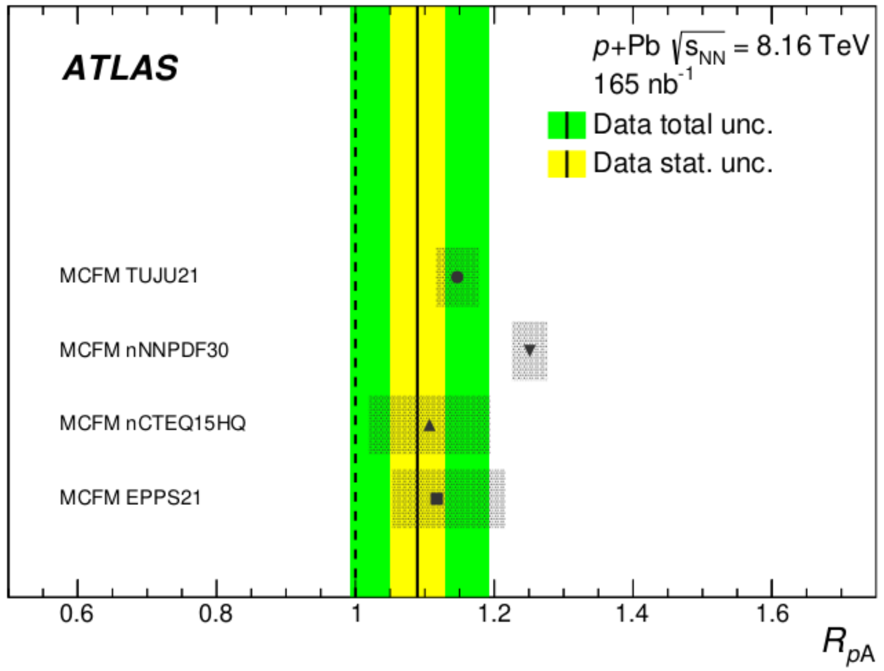

Summary

- Same-charge top-quark pair production (arXiv:2409.14982):
  - Placed upper limit on $\sigma(pp \to tt)$ and most stringent limits on WCs, **improving previous limits by factor $\approx$ 10**
- Inclusive cross-section $t\bar{t}$ + charm jets (arXiv:2409.11305)
  - Measured $t\bar{t} + \geq 2c$ and $t\bar{t} + 1c$ fiducial cross-sections that are **largely consistent with NLO+PS predictions** (NLO+PS underpredict by 0.5 to 2.0 standard deviations) and ratio of cross-sections that are **in agreement with POWHEG+PYTHIA8 simulations within 0.9 and 1.1 standard deviations**.
- $t\bar{t}$+ b-jets production in $e\mu$ final state (arXiv:2407.13473)
  - Integrated cross section measurements are **consistent with $t\bar{t}b\bar{b}$ predictions** within the uncertainties of the predictions.
- LFU in W-boson decays to e, μ (arXiv:2403.02133)
  - Results consistent with LFU **and higher precision results than previous world average**.
- $t\bar{t}$ production in p+Pb collisions (arXiv:2405.05078)
  - **Observation of $t\bar{t}$ process in p+Pb collisions by ATLAS** with **most precise $t\bar{t}$ cross-section** measured in nuclear collisions to date

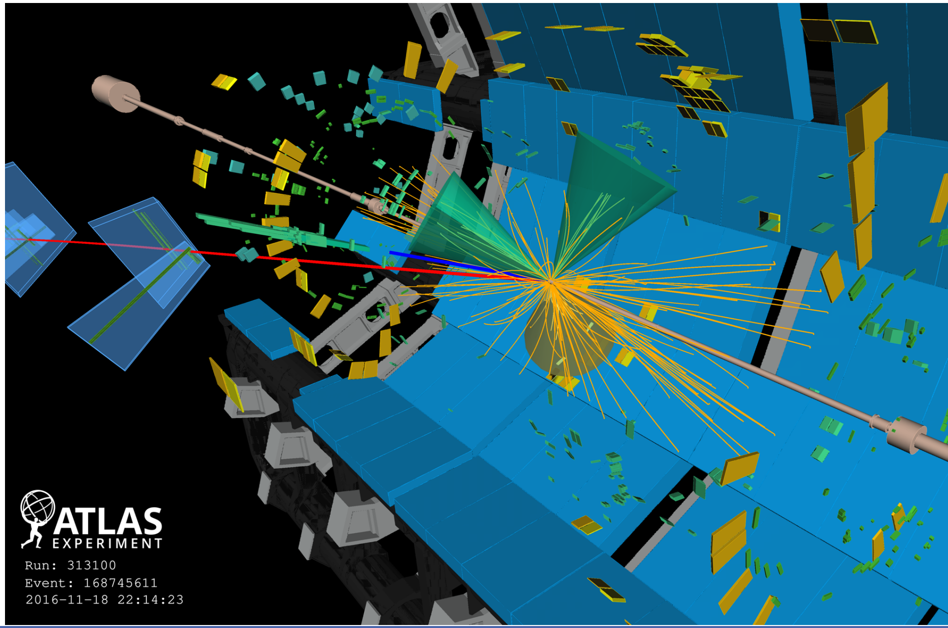

Thanks!

Highlights on top quark physics with the ATLAS experiment at the LHC

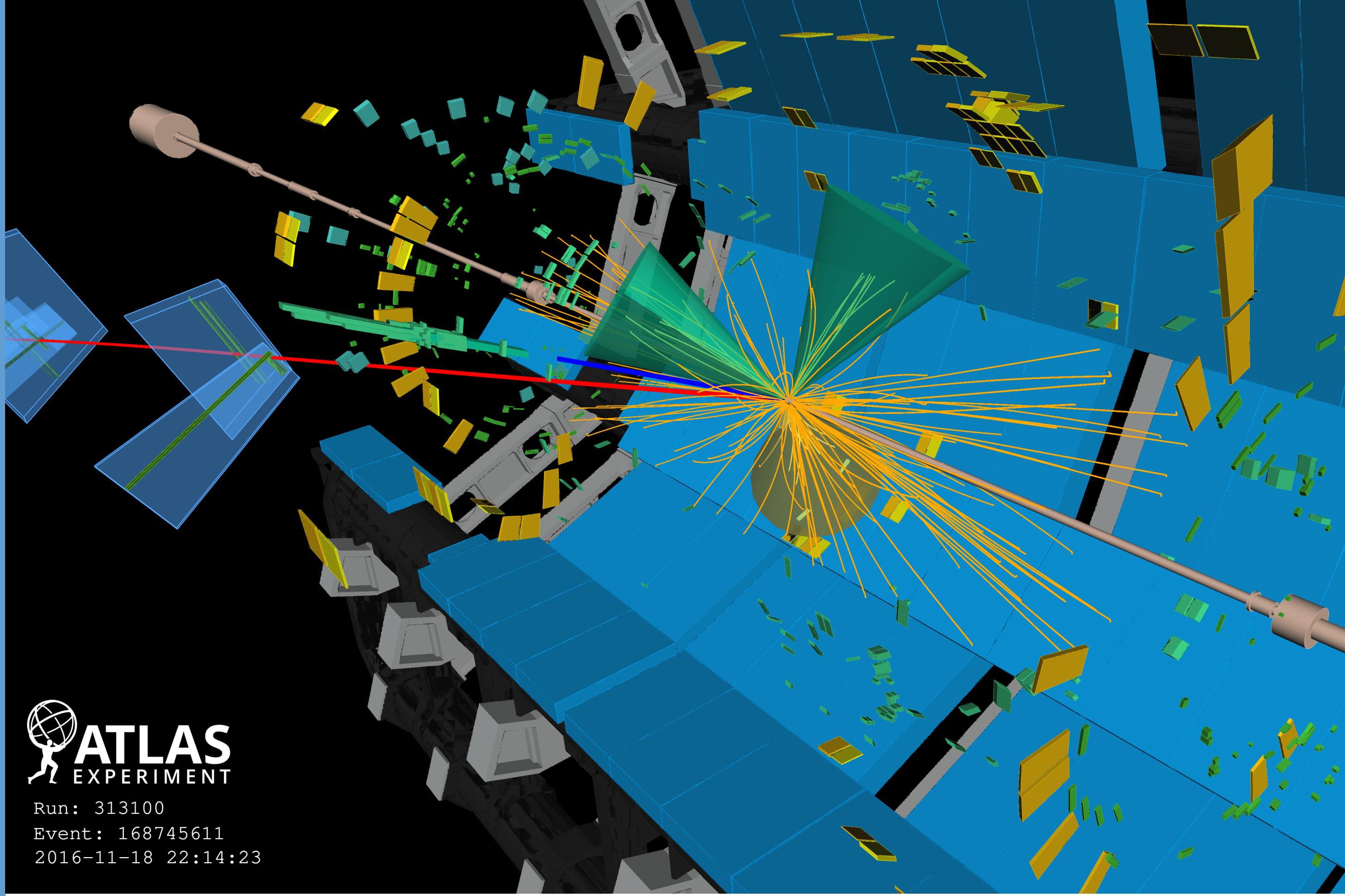

DEMOKRITOS

ROYAL HOLLOWAY UNIVERSITY OF LONDON

ATLAS EXPERIMENT

Back-up

arXiv:2409.14982

Same-charge top-quark pair production

- Three four-fermion operators are considered:
  - $O_{tu}^{(1)} = [\bar{t}_R \gamma^\mu u_R][\bar{t}_R \gamma_\mu u_R]$
  - $O_{Qu}^{(1)} = [\bar{Q}_L \gamma^\mu q_L][\bar{t}_R \gamma_\mu u_R]$
  - $O_{Qu}^{(8)} = [\bar{Q}_L \gamma^\mu T^A q_L][\bar{t}_R \gamma_\mu T^A u_R]$
  - Where Q_L and t_R are the left-handed doublet and right-handed singlet of the third quark generation, q_L and u_R are related to the first two generations and T^A is the generator of $SU(3)_C$
  - Effective lagrangian:

$$\mathcal{L}_{D=6}^{qq\to tt} = \frac{1}{\Lambda^2}\left(c_{tu}^{(1)} O_{tu}^{(1)} + c_{Qu}^{(1)} O_{Qu}^{(1)} + c_{Qu}^{(8)} O_{Qu}^{(8)}\right) + h.c.$$

  - with Wilson Coefficients (WCs) $c_{tu}^{(1)} = 0.04$, $c_{Qu}^{(1)} = 0.1$, $c_{Qu}^{(8)} = 0.2$ and new physics energy scale $\Lambda = 1$ TeV

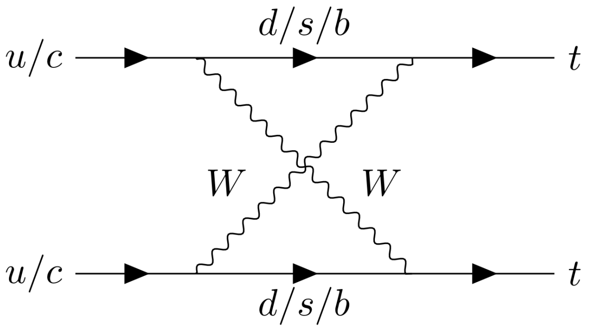

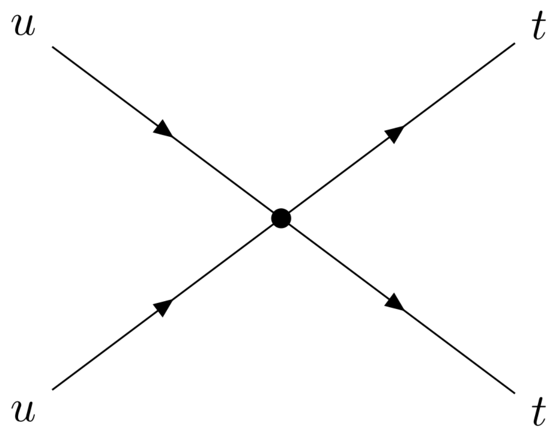

arXiv:2409.14982

Same-charge top-quark pair production

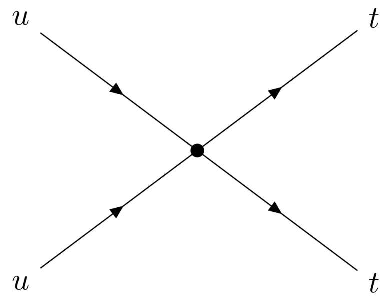

- Corresponds to cross-sections $\sigma(pp \to tt) = 97.6$ fb and $\sigma(pp \to \bar{t}\bar{t}) = 2.4$ fb $\to$ **highly charge asymmetric (tt production approx. 40 times larger).**
- tt events are produced by pairs of up or charm quarks (uu,uc,cc) while $\bar{t}\bar{t}$ events are produced via anti-up or anti-charm quarks ($\overline{uu}$, $\overline{uc}$, $\overline{cc}$) for the chosen EFT operators.
- The proton PDFs for reasonably high x, the ratio between up vs anti-up and anti-charm is of the order $\sim 20 - 30$

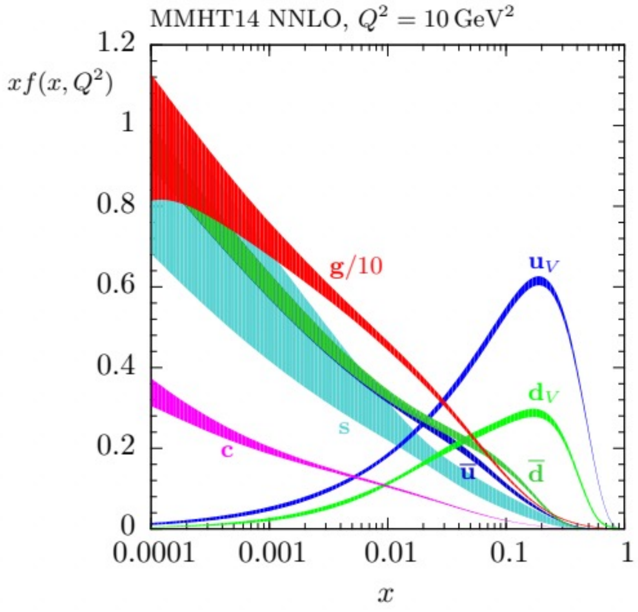

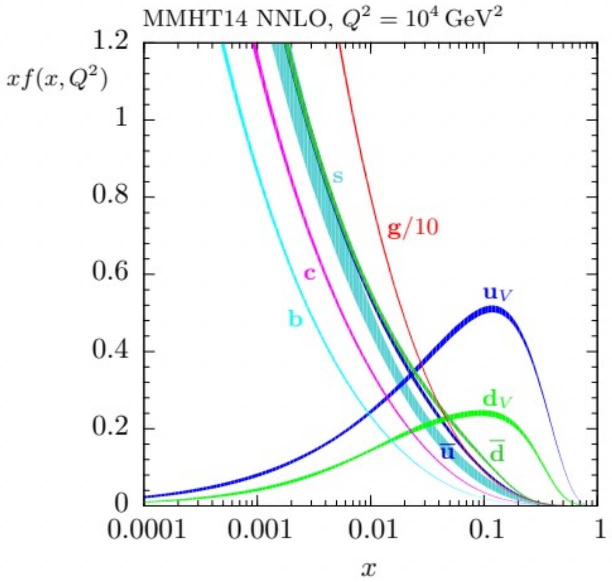

arXiv:2409.14982

Same-charge top-quark pair production

- NN^{SvsS} aim to discriminate between $c_{tu}^{(1)}$ vs $c_{Qu}^{(1)}$ or $c_{Qu}^{(8)}$
  - No further split between $c_{Qu}^{(1)}$ and $c_{Qu}^{(8)}$ due similarity in kinematic properties.
- Only trained on signal events
- Two signal samples used for training:
  - $c_{tu}^{(1)} = 0.04$, $c_{Qu}^{(1)} = 0$, $c_{Qu}^{(8)} = 0$
  - $c_{tu}^{(1)} = 0$, $c_{Qu}^{(1)} = 0.1$, $c_{Qu}^{(8)} = 0.2$
- Simple DNN with 5 hidden layers
- Using odd/even cross-validation
- 9 input variables ($\Delta\phi_{l,l}, \Delta R_{l,l}, \Delta\eta_{l,l}$, invariant mass of two-lepton system, scalar sum of the p_T of all jets, scalar sum of the p_T of all leptons, the p_T of the leading jet, E_T^{miss}, and the transverse mass of the combined lepton and E_T^{miss} system).
- Classification efficiency of 65% for both categories at 0.538 cut value on NN output
- The efficiency times acceptance values for signal events that enter the $SRtu$ and SR_{Qu} regions are 26.8% and 12.4% for signal events that originate from the $O^{(1)}_{tu}$ operator, and 15.8% and 19.5% for tu signal events that originate from the O_{Qu} operators.

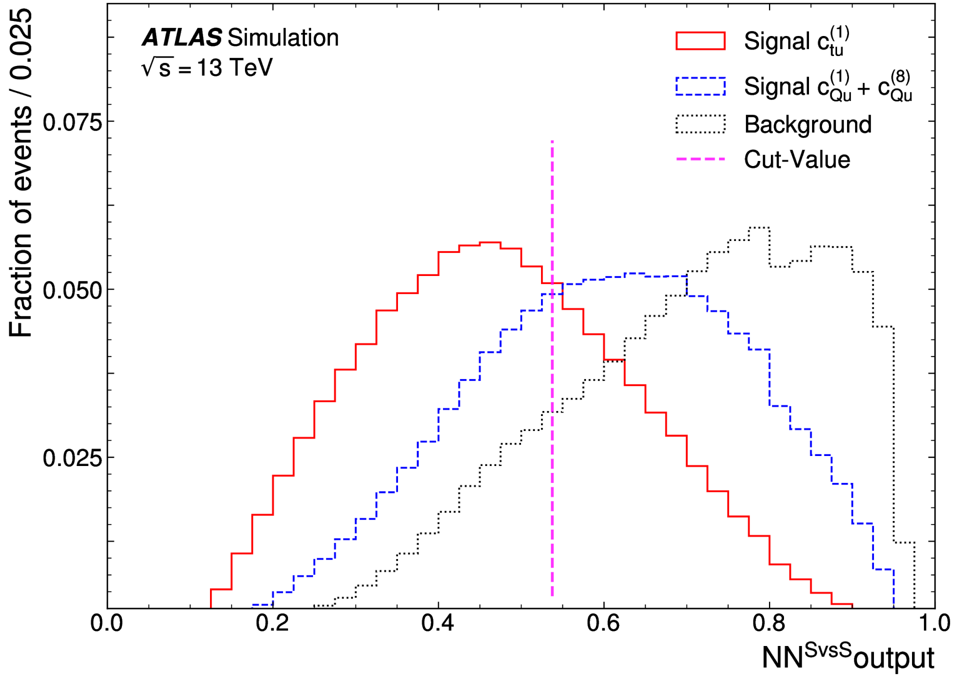

arXiv:2409.14982

Same-charge top-quark pair production

- NN^SvsB (aim to discriminate signal from background) has 6 kinematic quantities as input variables (sum of the p_T of all leptons, b-tagging score of leading and sub-leading p_T jets, p_T of leading jet, transverse mass of leptons and E_T^{miss} system, and number of jets in the event). Output used in profile likelihood fit for SRs.
- ttW has a known excess over theoretical predictions (that is in agreement with the ATLAS ttW cross-section measurement) – this background normalisation is therefore constrained in data.
  - Output of NN^SvsB is enriched in ttW events, especially in the first bins
  - Used for ttW normalisation
- Normalisations of other backgrounds from simulations, highest order perturbation theory calculations or from dedicated CRs

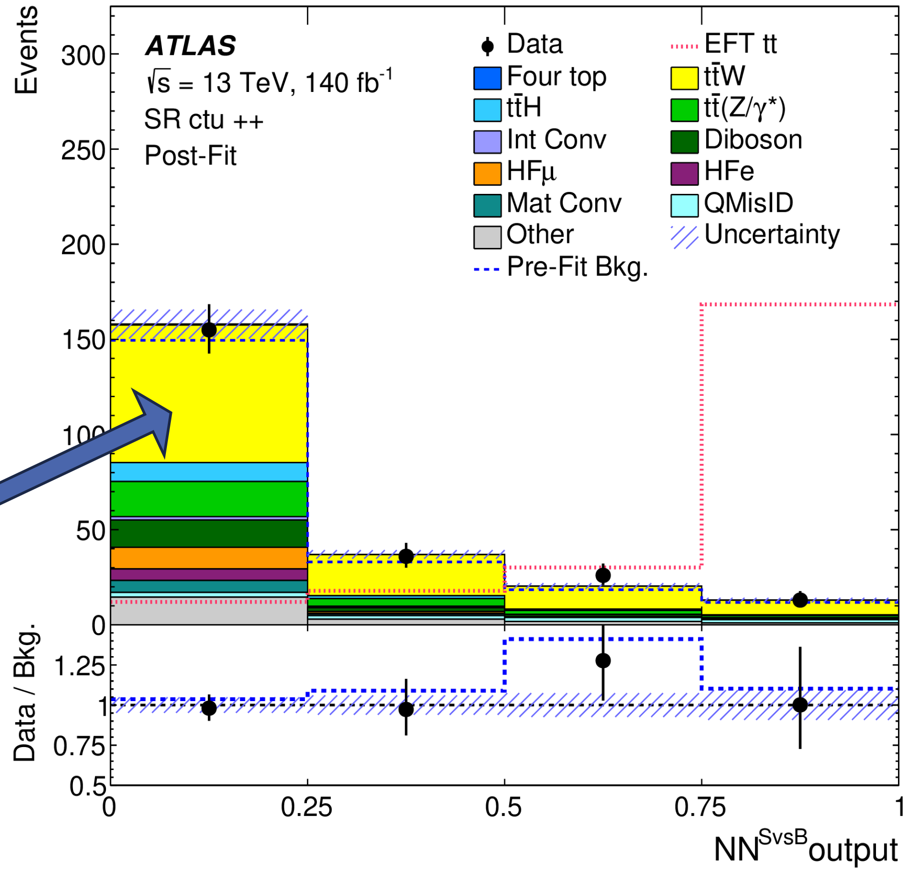

Same-charge top-quark pair pro

[arXiv:2409.14982]

- 9 CRs:
  - 5 dilepton CRs – enriched in HF e or mu fakes, orthogonal due to $N_{b\text{-tags}}$ and lepton isolation requirements
  - 4 three-lepton CRs – ttZ CR, diboson CR, photon conversion CRs, orthogonal due to requiring 3 leptons (electrons/muons)
- Good post-fit agreement in the CRs
- Normalisations of major bkg constrained by CRs
- For larger bkg, additional modelling uncertainties by comparing nominal MC with alternative sample
- All normalisations are in agreement with the SM, except ttW – this has a known excess that is in agreement with the ATLAS ttW cross-section measurement

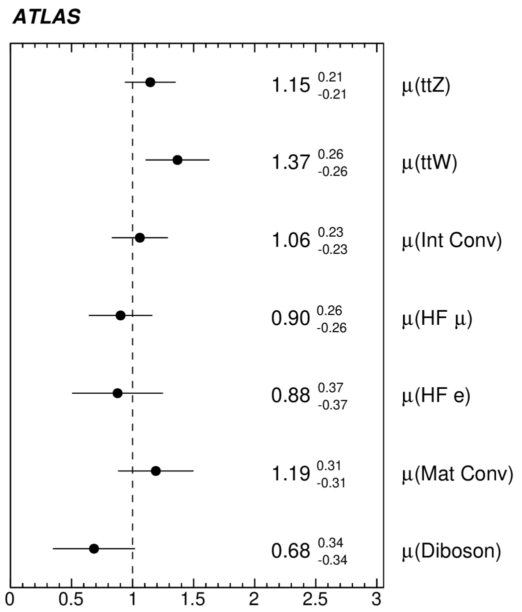

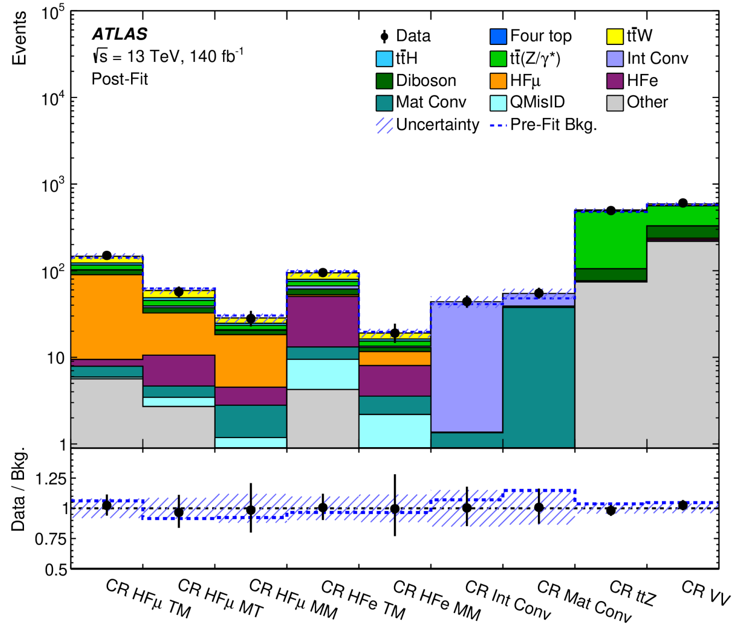

arXiv:2409.14982

Same-charge top-quark pair production

- Definitions of CRs

	CR HF TM	CR HF MT	CR HF MM
p_T^{lep} [GeV]		>20	
BDT WPs (same-sign ℓ pair)	TM	MT	MM
N_{jets}		≥2	
$N_{b-\text{tagged jets}}$		1 at 77%	
Total lepton charge		++ or - -	
m_T(all ℓ, E_T^{miss})	< 250 GeV		-

	VV CR	$t\bar{t}Z$ CR	CR Int Conv	CR Mat Conv
p_T^{lep} [GeV]		> 20 (SS pair), > 10 (OS)		
BDT WPs		$M_{inc}M_{inc}$ (SS pair) L_{inc} (OS)		
Total charge		±1		
Electron Conv. candidate		-	Int. Conv.	Mat. Conv.
N_{jets}	2 or 3	≥ 4	≥0	
$N_{b-\text{tagged jets}}$	1 b-tagged jet at 60% WP || ≥ 2 b-tagged jets at 77% WP		0 at 77%	
$\|m_{SFOS} - m_Z\|$	< 10 GeV		> 10 GeV	
$\|m(\ell\ell\ell) - m_Z\|$	-	-	< 10 GeV	

arXiv:2409.14982

Same-charge top-quark pair production

- CR yields - dilepton CRs

Process	CR HFμ TM	CR HFμ MT	CR HFμ MM	CR HFe TM	CR HFe MM
$t\bar{t}W$	24.0 ± 4.9	10.3 ± 2.0	3.73 ± 0.87	15.1 ± 2.9	2.76 ± 0.59
$t\bar{t}(Z/\gamma*)$	13.6 ± 2.1	6.20 ± 0.97	2.59 ± 0.47	8.4 ± 1.7	1.90 ± 0.32
$t\bar{t}H$	6.6 ± 4.0	3.2 ± 1.9	1.28 ± 0.79	4.1 ± 2.4	0.90 ± 0.58
Four top	0.113 ± 0.028	0.071 ± 0.017	0.046 ± 0.012	0.069 ± 0.019	0.036 ± 0.010
Diboson	11.9 ± 6.1	4.9 ± 2.5	2.2 ± 1.1	8.6 ± 4.4	1.35 ± 0.72
HFe	1.6 ± 1.1	5.9 ± 2.9	1.71 ± 0.97	37 ±12	4.5 ± 1.6
HFμ	80 ± 14	21.9 ± 5.6	13.8 ± 3.2	2.20 ± 0.66	3.62 ± 0.99
Mat Conv	2.0 ± 7.1	1.20 ± 0.56	1.62 ± 0.51	3.7 ± 2.1	1.38 ± 0.43
Int Conv	0.68 ± 0.41	1.7 ± 1.0	0.30 ± 0.18	5.5 ± 3.2	0.48 ± 0.30
QMisID	0.28 ± 0.13	0.75 ± 0.54	0.38 ± 0.26	5.2 ± 2.9	1.6 ± 1.0
Other	5.6 ± 1.5	2.71 ± 0.66	0.81 ± 0.21	4.2 ± 1.0	0.63 ± 0.16
Total Bkg.	147 ± 12	59.0 ± 5.1	28.4 ± 3.4	94.4 ± 9.2	19.1 ± 2.2
Data	150	57	28	95	19

arXiv:2409.14982

Same-charge top-quark pair production

- CR yields - three-lepton CRs

Process	CR Int Conv	CR Mat Conv	CR ttZ	CR VV
$t\bar{t}W$	–	–	8.4 ± 1.8	24.5 ± 4.7
$t\bar{t}(Z/\gamma*)$	–	–	378 ± 32	230 ± 27
$t\bar{t}H$	–	–	10.0 ± 6.3	6.3 ± 4.0
Four top	–	–	1.61 ± 0.32	0.092 ± 0.020
Diboson	0.025 ± 0.019	1.34 ± 0.72	29 ± 15	90 ± 45
HFe	–	–	0.47 ± 0.35	9.2 ± 6.8
HFμ	–	–	1.04 ± 0.35	7.5 ± 1.8
Mat Conv	1.3 ± 1.1	37.6 ± 8.6	0.59 ± 0.40	2.19 ± 0.77
Int Conv	42.5 ± 6.8	15.6 ± 4.3	0.14 ± 0.15	1.66 ± 0.96
QMisID	–	–	0.22 ± 0.17	0.83 ± 0.41
Other	–	–	74 ± 23	218 ± 40
Total Bkg.	43.9 ± 6.6	54.6 ± 7.3	503 ± 22	590 ± 23
Data	44	55	494	605

arXiv:2409.14982

Same-charge top-quark pair production

- SRs yields

Process	SR_{ctu++}	SR_{ctu--}	SR_{cQu++}	SR_{cQu--}
$t\bar{t}W$	114 ± 15	62 ± 10	110 ± 15	56.9 ± 9.0
$t\bar{t}(Z/\gamma*)$	25.5 ± 2.4	24.1 ± 2.6	19.5 ± 1.8	19.1 ± 1.8
$t\bar{t}H$	12.4 ± 7.5	12.3 ± 7.1	15.1 ± 9.6	15.1 ± 9.2
Four top	0.72 ± 0.15	0.69 ± 0.14	4.16 ± 0.83	4.07 ± 0.82
Diboson	18.1 ± 9.3	15.9 ± 8.1	6.3 ± 3.2	4.2 ± 2.1
HFe	6.5 ± 2.9	7.6 ± 3.0	3.0 ± 1.1	4.9 ± 2.5
HFμ	12.6 ± 2.7	15.7 ± 3.2	6.3 ± 1.8	5.7 ± 1.7
Mat Conv	7.6 ± 2.5	5.5 ± 1.6	2.73 ± 0.83	3.3 ± 1.2
Int Conv	2.7 ± 1.6	3.0 ± 1.7	2.1 ± 1.2	2.7 ± 1.6
QMisID	8.1 ± 2.2	8.1 ± 2.2	1.48 ± 0.39	1.48 ± 0.39
Other	20.3 ± 5.4	13.3 ± 3.9	9.3 ± 2.7	7.0 ± 2.6
Total Bkg.	228 ± 11	167.7 ± 7.9	180 ± 10	124.5 ± 6.3
Data	230	162	181	123

arXiv:2409.14982

Same-charge top-quark pair product

- Merged SR+VR

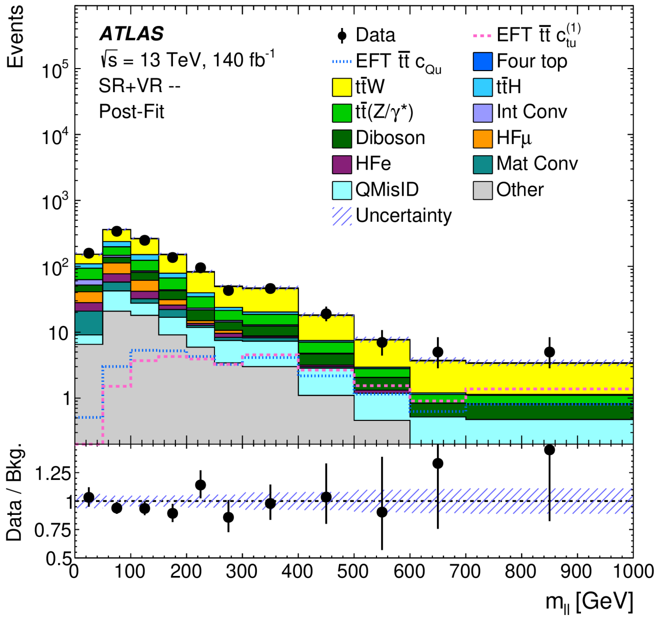

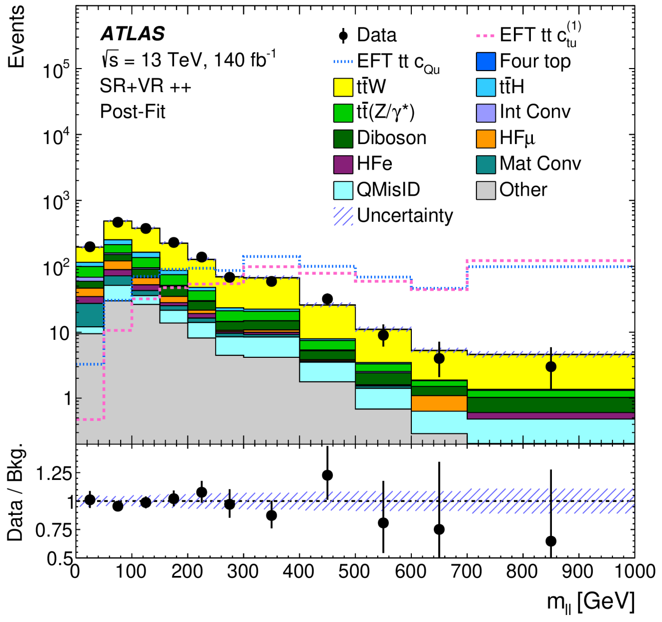

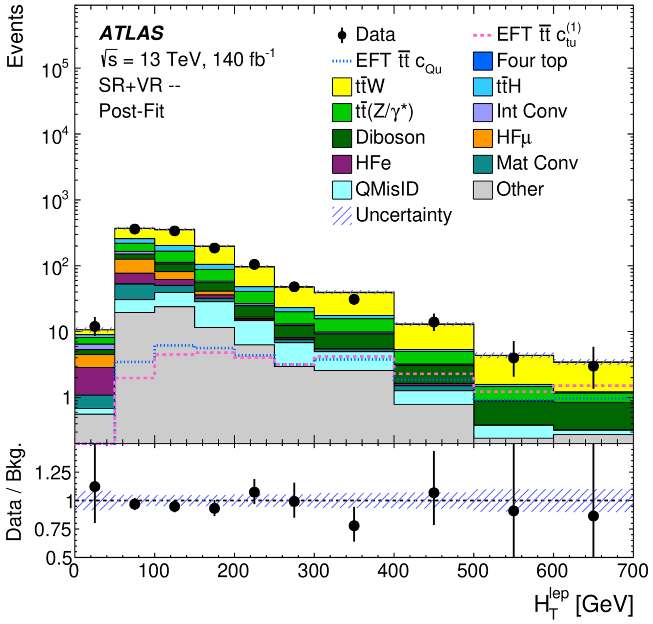

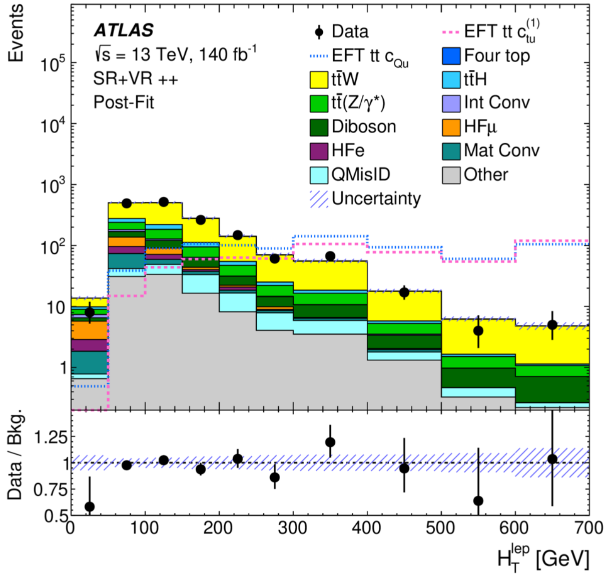

arXiv:2409.14982

Same-charge top-quark pair production

- Observed lower limits at 95% CL on scale of new physics, Λ for WC values 0.001, 1, $4\pi^2$

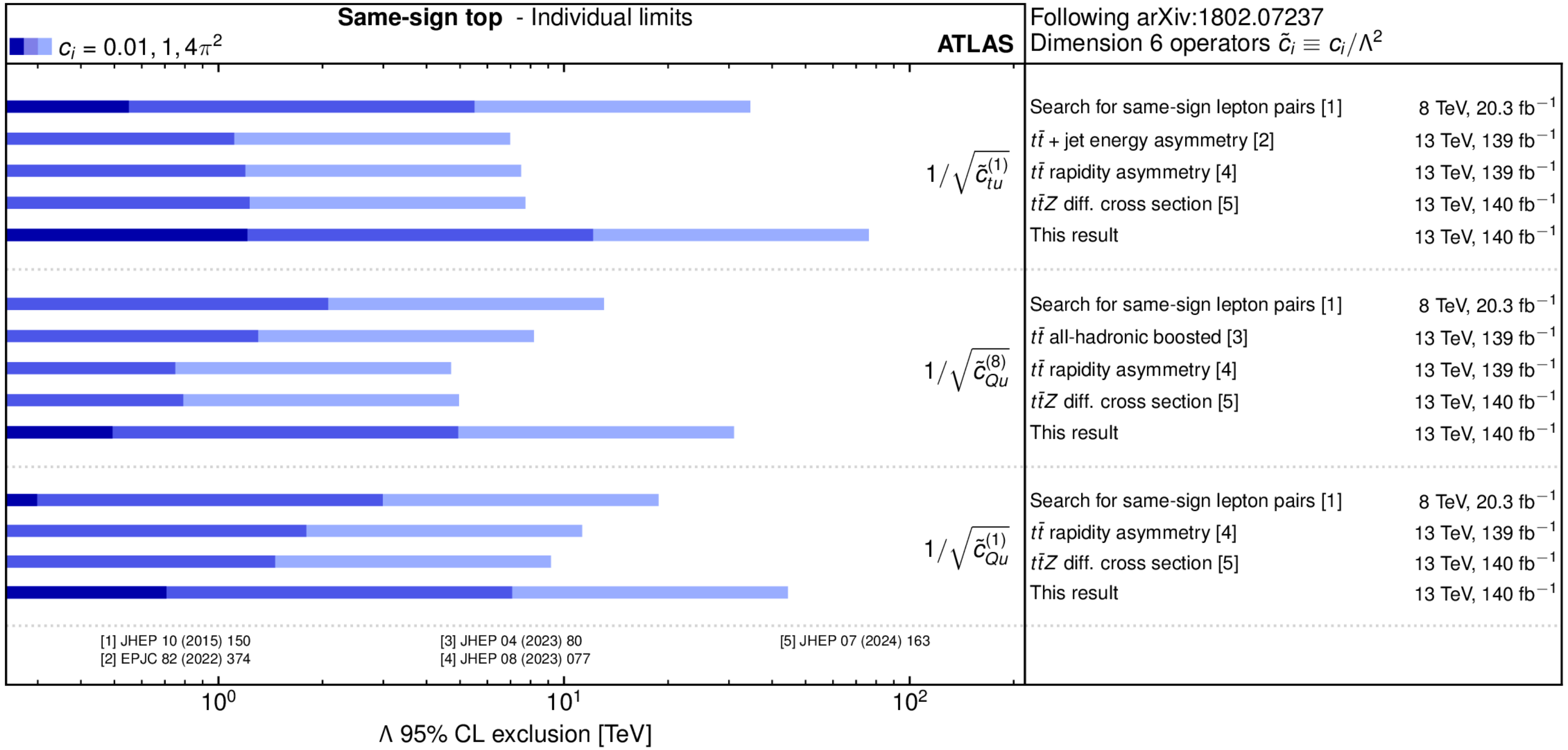

Same-charge top-quark pair production

- 2D limits for combinations of WCs

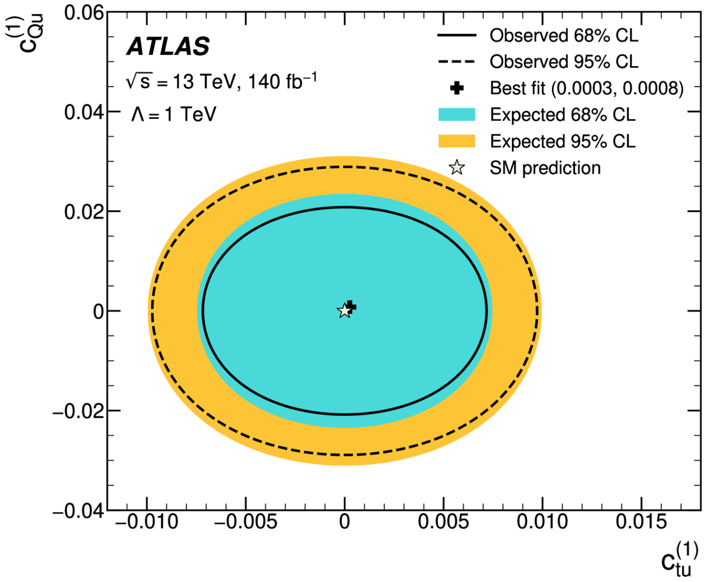

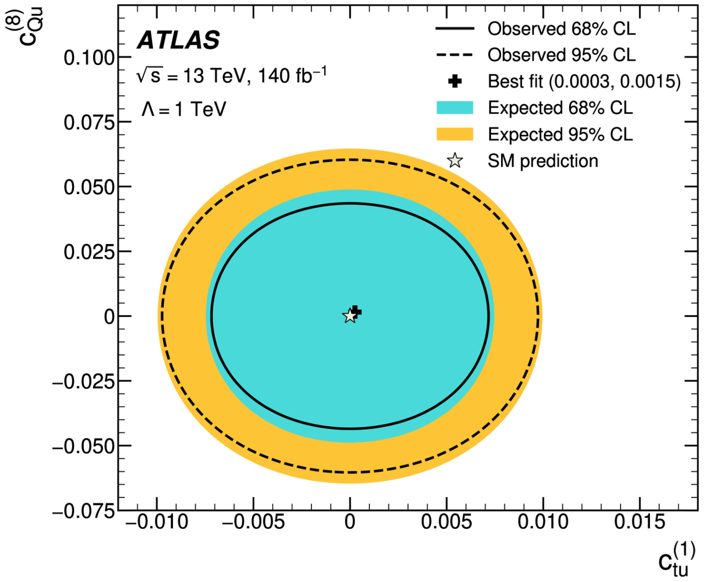

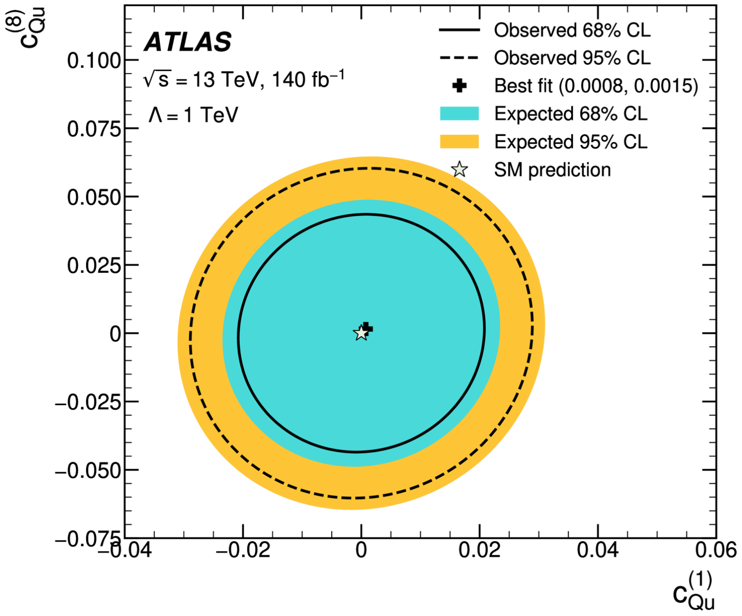

arXiv:2409.11305

Inclusive cross-section $t\bar{t}$ + charm jets

- Previous measurements
- tt+charm measurement by CMS in 2020
  - Uses 41.5 fb^{-1} of Run 2 data
  - Measured $t\bar{t} + c\bar{c}$ but did not explicitly measure $t\bar{t} + c/C$ cross-section
  - Showed agreement with NLO+PS MC predictions within one to two st dev of measurement uncertainties
- $t\bar{t} + b\bar{b}$,$t\bar{t}H(H \rightarrow b\bar{b})$ and $t\bar{t}t\bar{t}$ measurements determine the $t\bar{t} + \geq 1c$ normalisation in situ through a free parameter in the fit and recent results report this normalisation factor to be larger than MC predictions arXiv:2407.10904

arXiv:2409.11305

Inclusive cross-section $t\bar{t}$ + charm jets

- Event preselection
- 1L channel:
  - 1 charged lepton (e or μ)
  - ≥ 5 jets, ≥ 3 b/c-tagged (b@77% or c@22%)
  - Split into regions with 5 and ≥6 jets
- 2L channel:
  - 2 charged leptons (e or μ), opposite charge,
  - ≥ 3 jets, ≥ 2 b/c-tagged
  - Veto lepton pairs with m_{ll} < 15 GeV and close to Z-mass window
  - Split into regions with 3 and ≥ 4 jets
- Ratio measured in phase-space volume without requirements on the $t\bar{t}$ decay products and the jet multiplicity

arXiv:2409.11305

Inclusive cross-section $t\bar{t}$ + charm jets

- The ATLAS DL1r tagger outputs probabilities for the jet flavours: $p_b, p_c, p_{\text{light}}$ which is reoptimized as a 2D binned discriminant – the b/c tagger
- Axes of discriminant, D_c and D_b are calculated as weighted likelihood ratio of $p_b, p_c, p_{\text{light}}$ following the Neyman-Pearson lemma:

$$D_c = \log \frac{p_c}{f_b p_b + (1 - f_b) p_{\text{light}}}$$

- f_b, f_c control which background contributes more to the decision. It was found that f_b = 0.4 and f_c = 0.018 provide good performance for the b/c-tagger

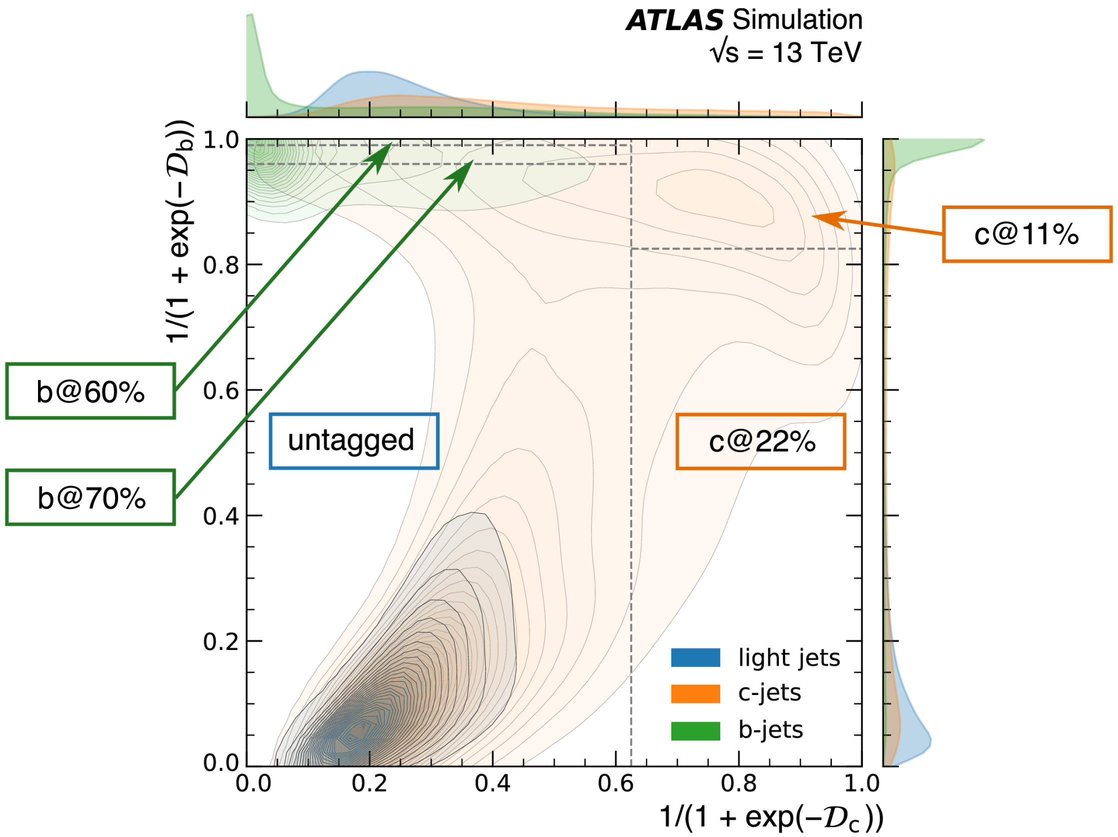

arXiv:2409.11305

Inclusive cross-section $t\bar{t}$ + charm jets

- The b/c-tagger at 5 WPs (including untagged bin dominated by light jets)

	Efficiency	c-jet rejection	light-jet rejection	$\mathcal{D}'_b$	$\mathcal{D}'_c$
b@60%	60.3%	37.1	2320	≥0.990	<0.625
b@70%	70.0%	12.2	573	≥0.963	<0.625

	Efficiency	b-jet rejection	light-jet rejection	$\mathcal{D}'_b$	$\mathcal{D}'_c$
c@11%	11.3%	28.7	1051	≥0.825	≥0.625
c@22%	22.4%	18.9	104	—	≥0.625

arXiv:2409.11305

Inclusive cross-section $t\bar{t}$ + charm jets

- CRs and SRs
  - 1L channel has additional c-quarks from W-boson decay

	$CR_1^{1\ell}$	$CR_2^{1\ell}$	$CR_3^{1\ell}$	$SR_{loose}^{1\ell}$	$SR_{tight}^{1\ell}$	$CR_1^{2\ell}$	$CR_2^{2\ell}$	$CR_3^{2\ell}$	$SR_{loose}^{2\ell}$	$SR_{tight}^{2\ell}$
N_{jets}	$= 5$ or ≥ 6					$= 3$ or ≥ 4				≥ 4
b@70%	2	–	–	2	2	2	–	≥ 3	2	2
b@60%	–	≥ 3	3	–	–	–	≥ 3	≤ 2	–	–
c@22%	1	0	1	≥ 2	–	0	–	–	1	≥ 2
c@11%	1	–	1	1	≥ 2	–	–	–	–	–

arXiv:2409.11305

Inclusive cross-section $t\bar{t}$ + charm jets

- Uncertainties on cross-sections

Uncertainty group	Fractional uncertainty [%] on $\sigma^{\text{fid}}(t\bar{t} + \geq 2c)$	$\sigma^{\text{fid}}(t\bar{t} + 1c)$
$t\bar{t} + \geq 1c$ modeling	9	8
Background modeling:		
$t\bar{t} + \geq 1b$	4	4
$t\bar{t}$ + light	6	4
Others	2.5	1.7
Instrumental:		
b-tagging	2.2	1.8
c-tagging	9	4
light mis-tagging	2.2	3.4
JES/JER	6	3.5
Others	1.3	0.9
MC statistics	3.1	2.5
Total systematic uncertainty	17	12
Data statistical uncertainty	11	7
Total	20	14

arXiv:2409.11305

Inclusive cross-section $t\bar{t}$ + charm jets

- Cross-section comparisons to MC simulations

	Measured	$t\bar{t}$ or $t\bar{t}+b\bar{b}$ Powheg+Pythia8
$\sigma^{\text{fid}}(t\bar{t}+\geq 1b)$ [pb]	3.46 ± 0.24	3.2 ± 1.6
$\sigma^{\text{fid}}(t\bar{t}+\geq 2c)$ [pb]	1.28 ± 0.25	1.04 ± 0.18
$\sigma^{\text{fid}}(t\bar{t}+1c)$ [pb]	6.4 ± 0.9	5.1 ± 0.8
$\sigma^{\text{inc}}(t\bar{t}+\geq 1b)$ [pb]	13.0 ± 0.9	12 ± 4
$\sigma^{\text{inc}}(t\bar{t}+\geq 2c)$ [pb]	5.4 ± 1.1	4.4 ± 0.7
$\sigma^{\text{inc}}(t\bar{t}+1c)$ [pb]	38 ± 6	31 ± 4
$R^{\text{fid}}_{t\bar{t}+\geq 1b}$ [%]	7.2 ± 0.4	6.5 ± 3.3
$R^{\text{fid}}_{t\bar{t}+\geq 2c}$ [%]	2.7 ± 0.5	2.1 ± 0.4
$R^{\text{fid}}_{t\bar{t}+1c}$ [%]	13.7 ± 1.8	10.3 ± 1.6
$R^{\text{inc}}_{t\bar{t}+\geq 1b}$ [%]	3.14 ± 0.23	2.6 ± 0.8
$R^{\text{inc}}_{t\bar{t}+\geq 2c}$ [%]	1.23 ± 0.25	0.97 ± 0.16
$R^{\text{inc}}_{t\bar{t}+1c}$ [%]	8.8 ± 1.3	6.9 ± 1.0

Inclusive cross-section $t\bar{t}$ + charm jets

- CRs and SRs regions post-fit

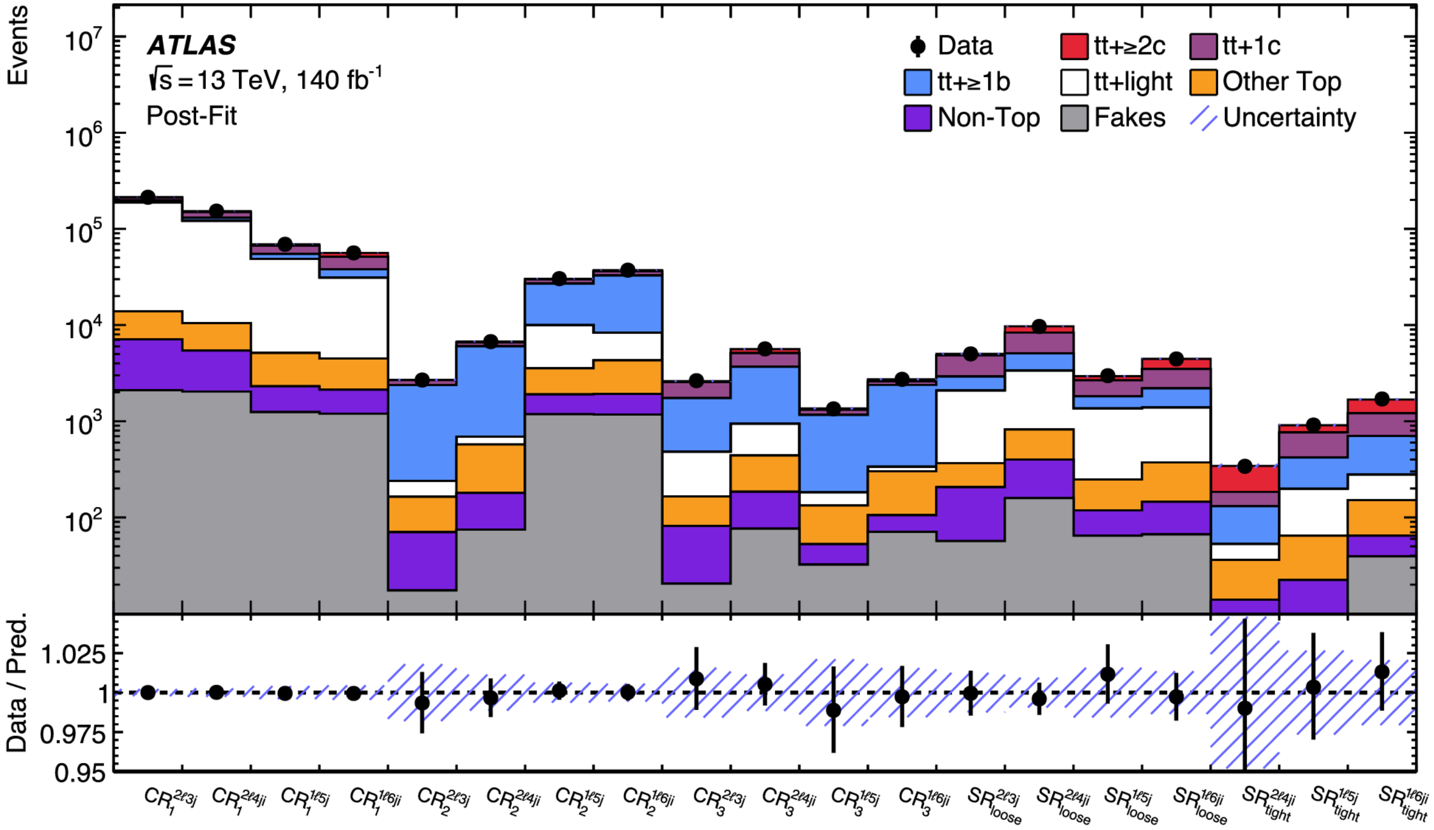

arXiv:2409.11305

Inclusive cross-sect a

- SRs regions post-fit

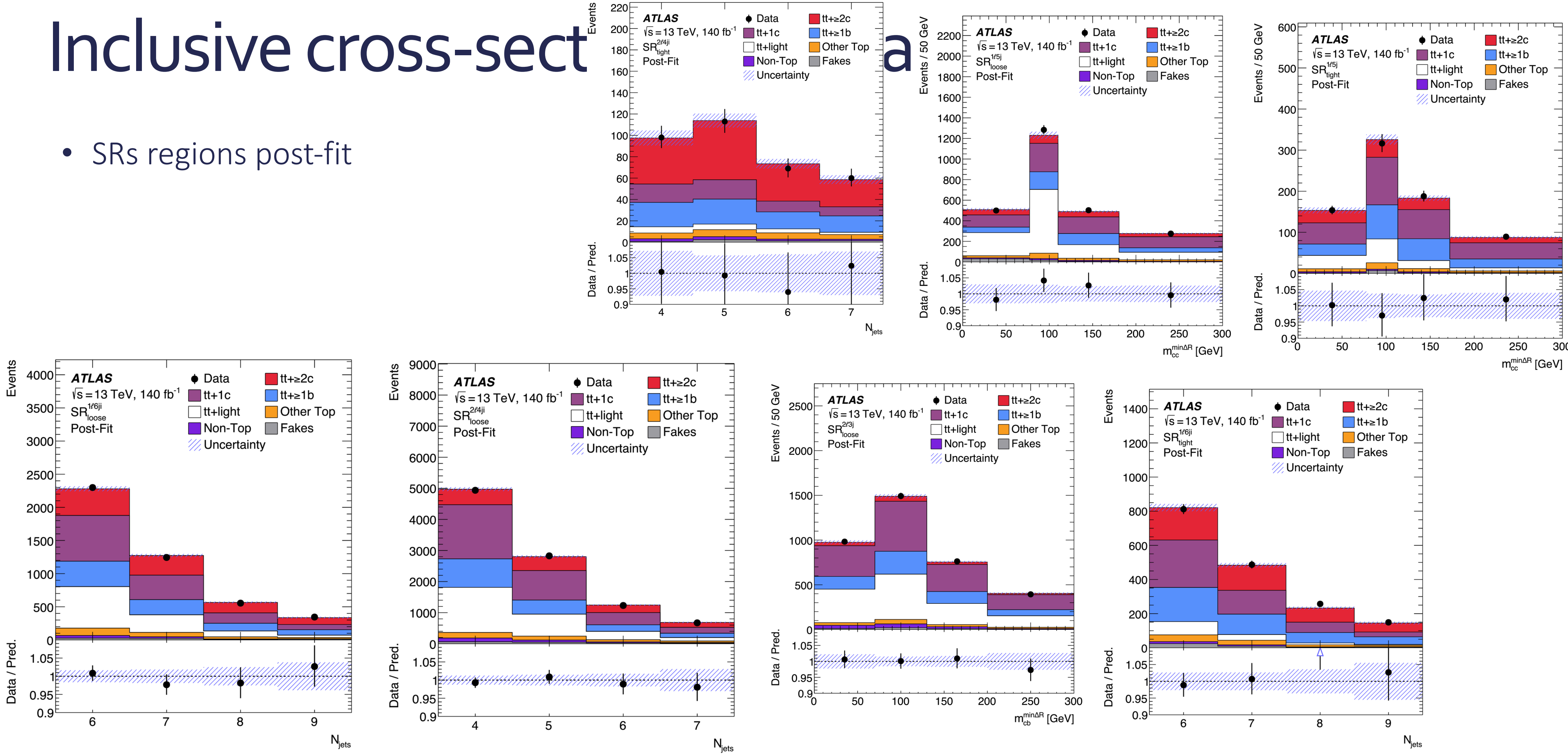

arXiv:2409.11305

Inclusive cross-section $t\bar{t}$ + charm jets

- Measured vs predicted cross-sections

	$t\bar{t}$ + ≥2c [pb]	$t\bar{t}$ + 1c [pb]	$t\bar{t}$ + ≥1b [pb]	$t\bar{t}$ + light [pb]	$t\bar{t}$ + jets [pb]
$t\bar{t}$ Powheg+Pythia 8	1.04 ± 0.18	5.1 ± 0.8	3.2 ± 0.5	40 ± 6	50 ± 7
$t\bar{t}$ Powheg+Pythia 8, $h_{\text{damp}} = 3\,m_t$	1.12 ± 0.16	5.4 ± 0.7	3.3 ± 0.5	41 ± 5	51 ± 7
$t\bar{t}$ Powheg+Pythia 8, $p_{\text{T}}^{\text{hard}} = 1$	1.05 ± 0.18	5.2 ± 0.8	3.1 ± 0.5	40 ± 6	50 ± 7
$t\bar{t}$ Powheg+Herwig 7	0.94 ± 0.16	4.2 ± 0.7	3.3 ± 0.5	43 ± 6	52 ± 8
$t\bar{t}$ MadGraph5_aMC@NLO+Herwig 7	0.74 ± 0.19	4.0 ± 0.8	2.7 ± 0.6	46 ± 8	53 ± 10
$t\bar{t} + b\bar{b}$ Powheg+Pythia 8	—	—	3.2 ± 1.6	—	—
$t\bar{t} + b\bar{b}$ Powheg+Pythia 8, $p_{\text{T}}^{\text{hard}} = 1$	—	—	2.8 ± 1.3	—	—
$t\bar{t} + b\bar{b}$ Powheg+Pythia 8, $h_{\text{bzd}} = 2$	—	—	3.1 ± 1.5	—	—
$t\bar{t} + b\bar{b}$ Powheg+Pythia 8, dipole recoil	—	—	3.0 ± 1.4	—	—
$t\bar{t} + b\bar{b}$ Powheg+Herwig 7	—	—	3.1 ± 1.6	—	—
$t\bar{t} + b\bar{b}$ Sherpa 2.2.10	—	—	3.5 ± 1.0	—	—
Data	1.28 ± 0.25	6.4 ± 0.9	3.46 ± 0.24	36.0 ± 1.8	47.1 ± 2.3

arXiv:2409.11305

Inclusive cross-section $t\bar{t}$ + charm jets

- Post-fit yields

	$CR_1^{1\ell5j}$	$CR_1^{1\ell6ji}$	$CR_2^{1\ell5j}$	$CR_2^{1\ell6ji}$	$CR_3^{1\ell5j}$	$CR_3^{1\ell6ji}$
$t\bar{t} + \geq 2c$	2300 ± 500	5000 ± 800	470 ± 110	1000 ± 190	47 ± 10	140 ± 21
$t\bar{t} + 1c$	12 100 ± 1900	13 400 ± 1600	2900 ± 400	3500 ± 400	149 ± 16	209 ± 23
$t\bar{t} + \geq 1b$	6000 ± 330	6800 ± 330	16 900 ± 700	24 400 ± 900	980 ± 40	2050 ± 80
$t\bar{t}$ + light	43 600 ± 1900	26 700 ± 1600	6460 ± 320	4020 ± 330	50 ± 11	34 ± 15
Other Top	2800 ± 600	2400 ± 500	1700 ± 400	2400 ± 600	80 ± 22	200 ± 60
Non-Top	1100 ± 400	930 ± 350	720 ± 260	750 ± 280	20 ± 8	34 ± 13
Fakes	1200 ± 600	1200 ± 500	1200 ± 500	1200 ± 500	32 ± 18	71 ± 35
Total	69 170 ± 280	56 310 ± 260	30 350 ± 190	37 200 ± 210	1360 ± 29	2740 ± 40
Data	69 136	56 277	30 388	37 209	1345	2728

	$CR_1^{2\ell3j}$	$CR_1^{2\ell4ji}$	$CR_2^{2\ell3j}$	$CR_2^{2\ell4ji}$	$CR_3^{2\ell3j}$	$CR_3^{2\ell4ji}$
$t\bar{t} + \geq 2c$	1130 ± 270	3600 ± 800	21 ± 5	168 ± 34	62 ± 14	520 ± 90
$t\bar{t} + 1c$	14 500 ± 1800	18 900 ± 2300	307 ± 33	560 ± 50	810 ± 80	1420 ± 140
$t\bar{t} + \geq 1b$	8500 ± 800	8900 ± 600	2130 ± 70	5330 ± 160	1260 ± 60	2740 ± 120
$t\bar{t}$ + light	175 100 ± 2700	111 000 ± 2700	75 ± 10	117 ± 20	320 ± 40	500 ± 70
Other Top	6800 ± 1200	5100 ± 1100	94 ± 29	390 ± 110	84 ± 20	260 ± 60
Non-Top	5000 ± 1700	3400 ± 1100	53 ± 18	105 ± 35	61 ± 22	110 ± 40
Fakes	2100 ± 500	2000 ± 500	17 ± 4	75 ± 19	20 ± 5	76 ± 19
Total	213 200 ± 500	152 900 ± 400	2700 ± 50	6750 ± 80	2620 ± 40	5630 ± 70
Data	213 185	152 931	2682	6725	2640	5655

arXiv:2409.11305

Inclusive cross-section $t\bar{t}$ + charm jets

- Post-fit yields

	$SR^{2\ell 3j}_{loose}$	$SR^{2\ell 4ji}_{loose}$	$SR^{1\ell 5j}_{loose}$	$SR^{1\ell 6ji}_{loose}$	$SR^{2\ell 4ji}_{tight}$	$SR^{1\ell 5j}_{tight}$	$SR^{1\ell 6ji}_{tight}$
$t\bar{t} + \geq 2c$	190 ± 40	1350 ± 220	280 ± 50	960 ± 140	159 ± 22	144 ± 26	470 ± 70
$t\bar{t} + 1c$	1910 ± 180	3270 ± 330	850 ± 90	1300 ± 150	54 ± 8	347 ± 32	510 ± 60
$t\bar{t} + \geq 1b$	830 ± 40	1710 ± 70	450 ± 26	810 ± 50	77 ± 5	220 ± 13	425 ± 22
$t\bar{t}$ + light	1720 ± 160	2540 ± 250	1120 ± 90	1020 ± 140	17 ± 5	134 ± 28	127 ± 34
Other Top	160 ± 40	420 ± 80	130 ± 40	230 ± 50	22 ± 6	42 ± 9	87 ± 24
Non-Top	150 ± 50	240 ± 80	54 ± 20	78 ± 30	8 ± 3	14 ± 5	25 ± 9
Fakes	57 ± 14	160 ± 40	64 ± 32	70 ± 40	6 ± 2	8 ± 6	39 ± 20
Total	5020 ± 60	9710 ± 90	2940 ± 50	4460 ± 60	343 ± 16	910 ± 24	1683 ± 35
Data	5015	9668	2976	4443	340	913	1705

arXiv:2409.11305

Inclusive cross-section $t\bar{t}$ + charm jets

- Nuisance parameter ranking
- $\sigma^{\text{fid}}(t\bar{t} + \geq 2c)$

$\sigma^{\text{fid}}(t\bar{t} + 1c)$

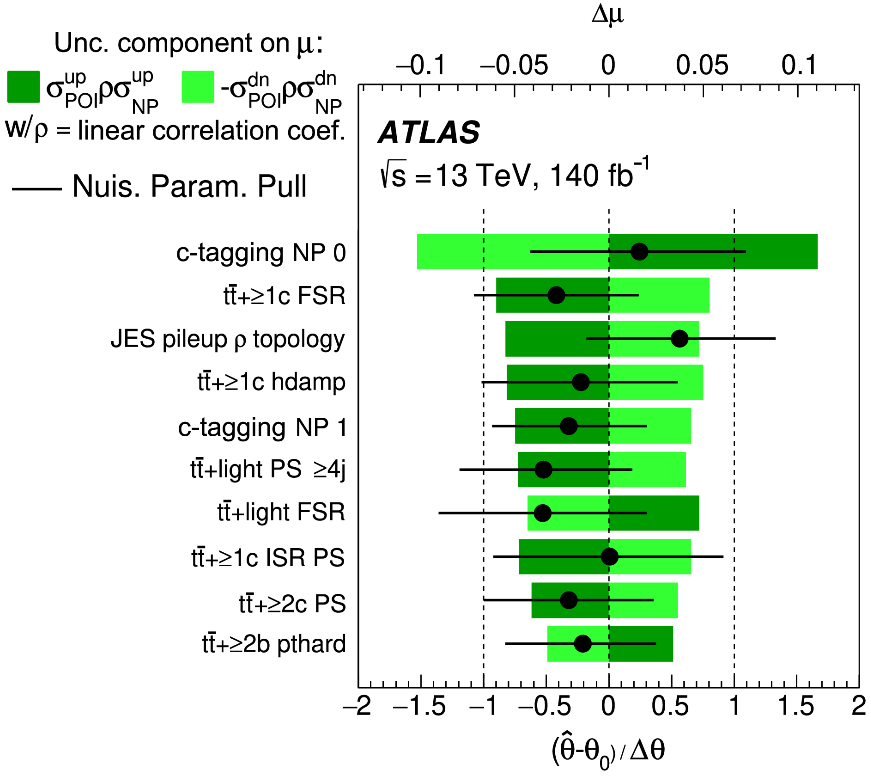

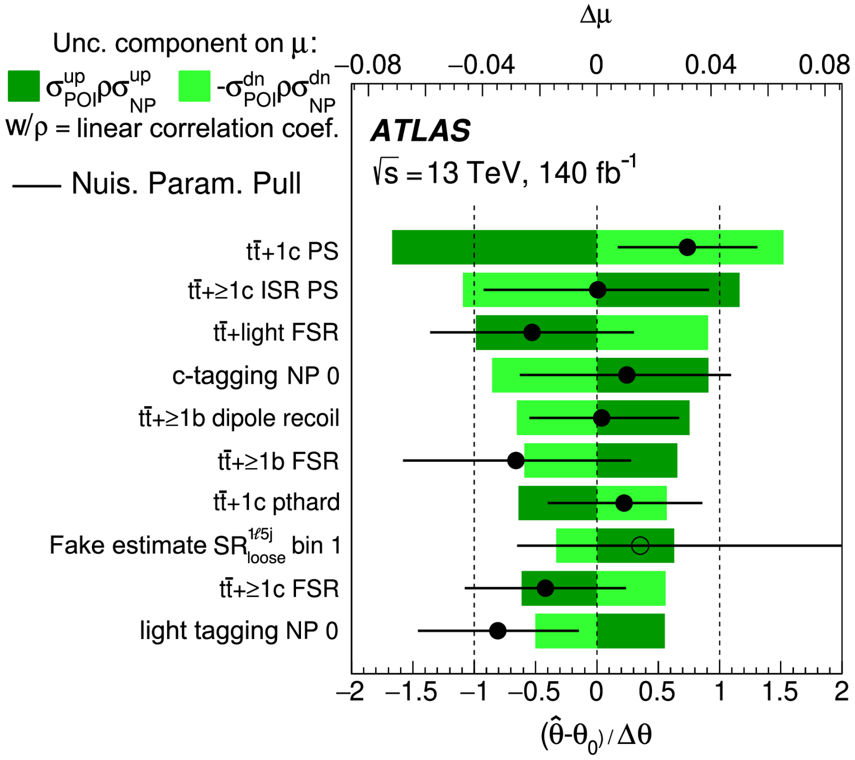

arXiv:2409.11305

Inclusive cross-section $t\bar{t}$ + charm jets

- Nuisance parameter ranking
- $R^{\text{fid}}_{t\bar{t}+\geq 2c}$

$R^{\text{fid}}_{t\bar{t}+1c}$

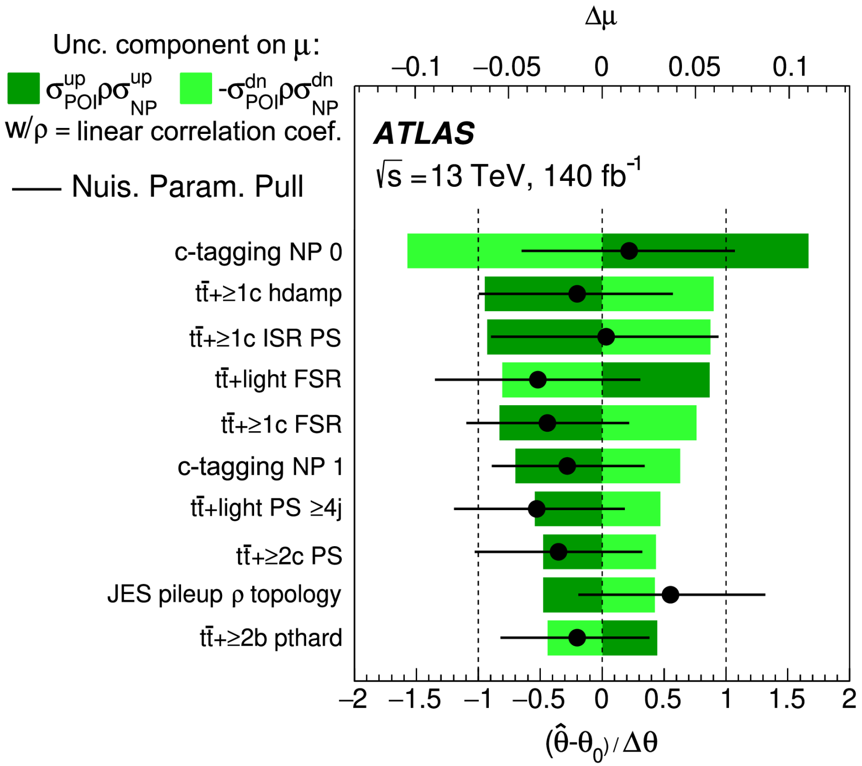

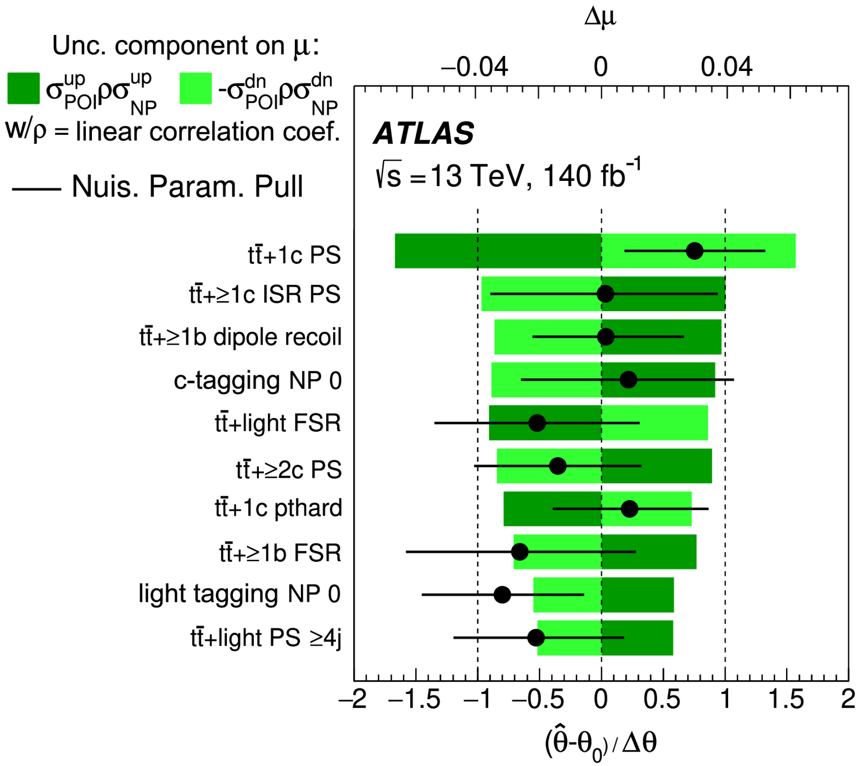

$t\bar{t}$+ b-jets production in $e\mu$ final state

- Previous Results
  - Previous ATLAS measurements of $t\bar{t}$ +b-jets all found the MC simulations to underpredict the measured results arXiV:1304.6386, arXiv:1508.06868, arXiv:1811.12113
  - Recent $t\bar{t}b\bar{b}$ measurements by CMS Collaboration in semileptonic decay channel using the full 13 TeV data sample, found the data exceeded the predictions of several MC simulations arXiv:2309.14442

arXiv:2407.13473

$t\bar{t}$+ b-jets production in $e\mu$ final state

MC sample	Generator	Process	Parton shower	Matching/ Parton shower settings	Tune	Use
Powheg+Pythia8	Powheg Box v2	$t\bar{t}$ NLO	Pythia 8.230	Powheg h_{damp} =1.5m_{top} p_T^{hard} = 0 globalRecoil recoilToColoured=ON	A14	nom.
Powheg+Pythia8 h_{damp}	Powheg Box v2	$t\bar{t}$ NLO	Pythia 8.230	Powheg h_{damp} =3m_{top}	A14	syst.
Powheg+Pythia8 p_T^{hard}	Powheg Box v2	$t\bar{t}$ NLO	Pythia 8.230	Powheg p_T^{hard} = 1	A14	syst.
Powheg+Pythia8 RecoilToTop	Powheg Box v2	$t\bar{t}$ NLO	Pythia 8.230	Powheg recoilToTop	A14	syst.
Powheg+Herwig 7	Powheg Box v2	$t\bar{t}$ NLO	Herwig 7.1.3	Powheg	H7.1-Default	syst.
Powheg+Pythia8 dipole	Powheg Box v2	$t\bar{t}$ NLO	Pythia 8.230	Powheg dipoleRecoil on	A14	comp.
MadGraph5_aMC@NLO+Pythia 8	MadGraph5_ aMC@NLO v2.6.0	$t\bar{t}$ NLO	Pythia 8.230	MC@NLO	A14	comp.
MadGraph5_aMC@NLO+Herwig 7	MadGraph5_ aMC@NLO v2.6.0	$t\bar{t}$ NLO	Herwig 7.1.3	MC@NLO	H7.1-Default	comp.
Sherpa	Sherpa 2.2.12	$t\bar{t}$ +0,1 parton at NLO +2,3,4 parton at LO	Sherpa	MePs@Nlo	Author's tune	comp.
Powheg+Pythia8 $t\bar{t}b\bar{b}$	Powheg Box Res	$t\bar{t}b\bar{b}$ NLO	Pythia 8.230	Powheg Box Res h_{bzd}=5 p_T^{hard} = 0 globalRecoil	A14	comp.
Powheg+Pythia8 $t\bar{t}b\bar{b}$ p_T^{hard}	Powheg Box Res	$t\bar{t}b\bar{b}$ NLO	Pythia 8.230	Powheg Box Res p_T^{hard} = 1	A14	comp.
Powheg+Pythia8 $t\bar{t}b\bar{b}$ h_{bzd}	Powheg Box Res	$t\bar{t}b\bar{b}$ NLO	Pythia 8.230	Powheg Box Res h_{bzd}=2	A14	comp.
Powheg+Pythia8 $t\bar{t}b\bar{b}$ dipole	Powheg Box Res	$t\bar{t}b\bar{b}$ NLO	Pythia 8.230	Powheg Box Res h_{bzd}=2 dipoleRecoil on	A14	comp.
Powheg+Herwig 7 $t\bar{t}b\bar{b}$	Powheg Box Res	$t\bar{t}b\bar{b}$ NLO	Herwig 7.1.6	Powheg Box Res	H7.1-Default	comp.
Sherpa $t\bar{t}b\bar{b}$	Sherpa 2.2.10	$t\bar{t}b\bar{b}$ NLO	Sherpa	MePs@Nlo	Author's tune	comp.
Helac-NLO (off-shell)	Helac-NLO	$e\mu$ + 4b NLO	–	–	–	comp.

arXiv:2407.13473

$t\bar{t}$+ b-jets production in $e\mu$ final state

Observable	Description	Phase spaces				
		$\geq 2b$	$\geq 3b$	$\geq 3b$ $\geq 1l/c$	$\geq 4b$	$\geq 4b$ $\geq 1l/c$
σ^{fid}	Fiducial total cross-section		✓	✓	✓	✓
$N_{b\text{-jets}}$	Number of b-jets	✓	✓			
$N_{l/c\text{-jets}}$	Number of light- or c-jets		✓		✓	
$H_{\text{T}}^{\text{had}}$	Scalar sum of p_{T} of all jets		✓		✓	
$H_{\text{T}}^{\text{all}}$	Scalar sum of p_{T} of charged leptons, jet and missing E_{T}		✓		✓	
$\Delta R_{\text{avg}}^{bb}$	Average angular distance in ΔR of b-jet pairs		✓		✓	
$\Delta\eta_{\text{max}}^{jj}$	Maximum absolute difference in η between any pair of jets		✓		✓	
$p_{\text{T}}(b_1)$	p_{T} of the hardest b-jet		✓		✓	
$p_{\text{T}}(b_2)$	p_{T} of second-hardest b-jet		✓		✓	
$p_{\text{T}}(b_3)$	p_{T} of third-hardest b-jet		✓		✓	
$p_{\text{T}}(b_4)$	p_{T} of fourth-hardest b-jet				✓	
$\eta(b_1)$	η of hardest b-jet		✓		✓	
$\eta(b_2)$	η of second-hardest b-jet		✓		✓	
$\eta(b_3)$	η of third-hardest b-jet		✓		✓	
$\eta(b_4)$	η of fourth-hardest b-jet				✓	
$p_{\text{T}}(l/c\text{-jet}_1)$	p_{T} of the hardest light- or c-jet			✓		✓
$\eta(l/c\text{-jet}_1)$	η of the hardest light- or c-jet			✓		✓
$m(b_1b_2)$	Invariant mass of two hardest b-jets in p_{T}		✓		✓	
$\Delta R(b_1, b_2)$	ΔR between two hardest b-jets		✓		✓	
$p_{\text{T}}(b_1b_2)$	p_{T} of two hardest b-jets		✓		✓	
$m(bb^{\min\Delta R})$	Invariant mass of two closest b-jets in ΔR				✓	
$p_{\text{T}}(bb^{\min\Delta R})$	p_{T} of the closest b-jets pair				✓	
$\min\Delta R(bb)$	Closest angular distance in ΔR among b-jets				✓	
$m(e\mu b_1b_2)$	Invariant mass of electron, muon and two hardest b-jets		✓		✓	
$p_{\text{T}}(b_1^{\text{top}})$	p_{T} of the hardest b-jet assigned to top quark		✓		✓	
$p_{\text{T}}(b_2^{\text{top}})$	p_{T} of the second-hardest b-jet assigned to top quark		✓		✓	
$p_{\text{T}}(b_1^{\text{add}})$	p_{T} of the hardest additional b-jet		✓		✓	
$p_{\text{T}}(b_2^{\text{add}})$	p_{T} of the second-hardest additional b-jet				✓	
$\eta(b_1^{\text{top}})$	η of the hardest b-jet assigned to top quark		✓		✓	
$\eta(b_2^{\text{top}})$	η of the second-hardest b-jet assigned to top quark		✓		✓	
$\eta(b_1^{\text{add}})$	η of the hardest additional b-jet		✓		✓	
$\eta(b_2^{\text{add}})$	η of the second-hardest additional b-jet				✓	
$m(bb^{\text{top}})$	Invariant mass of a pair of b-jets assigned to top quarks		✓		✓	
$p_{\text{T}}(bb^{\text{top}})$	p_{T} of a pair of b-jets assigned to top quarks		✓		✓	
$m(bb^{\text{add}})$	Invariant mass of a pair of additional b-jets				✓	
$p_{\text{T}}(bb^{\text{add}})$	p_{T} of a pair of additional b-jets				✓	
$m(e\mu bb^{\text{top}})$	Invariant mass of $e\mu$ and the b-jets pair assigned to top quarks		✓		✓	
$\Delta R(e\mu bb^{\text{top}}, b_1^{\text{add}})$	ΔR between the direction of the system of $e\mu$ and b-jet pair assigned to top and the direction of the hardest additional b-jet		✓		✓	
$\Delta R(e\mu bb^{\text{top}}, l/c\text{-jet}_1)$	ΔR between the direction of the system of $e\mu$ and b-jet pair assigned to top and the direction of the hardest light- or c-jet			✓		✓
$p_{\text{T}}(l/c\text{-jet}_1) - p_{\text{T}}(b_1^{\text{add}})$	Difference in p_{T} between the hardest l/c-jet and the additional b-jet			✓		✓

arXiv:2407.13473

$t\bar{t}$+ b-jets production in $e\mu$ final state

- Template fit for mistagged jets in $t\bar{t}$+light and $t\bar{t}$+c events – two fits are performed:
  - Global fit:
    - fitting normalisation factors for $t\bar{t}$+b, $t\bar{t}$+c, $t\bar{t}$+l templates in the inclusive region
    - Nominal approach to correct the normalisation of individual $t\bar{t}j$ components
  - Kinematic-dependent fit:
    - fitting normalisation factors in the specific regions depending on overall jet multiplicity and pT ranges of 3rd hardest jet in the reconstructed events
    - Used to evaluate systematic uncertainties due to shape effects of $t\bar{t}c$ and $t\bar{t}l$ background

Detector level event selection:

- Exactly one electron and one muon – OS, $p_T >$ 28 GeV, $|\eta| < 2.5$, $m_{e\mu} > 15$ GeV to reject low-mass τ
- $\geq$ 2 jets, $p_T >$ 25 GeV, $|\eta| < 2.5$
- $\geq$ 2 b-jets, DL1r at 77% efficiency WP

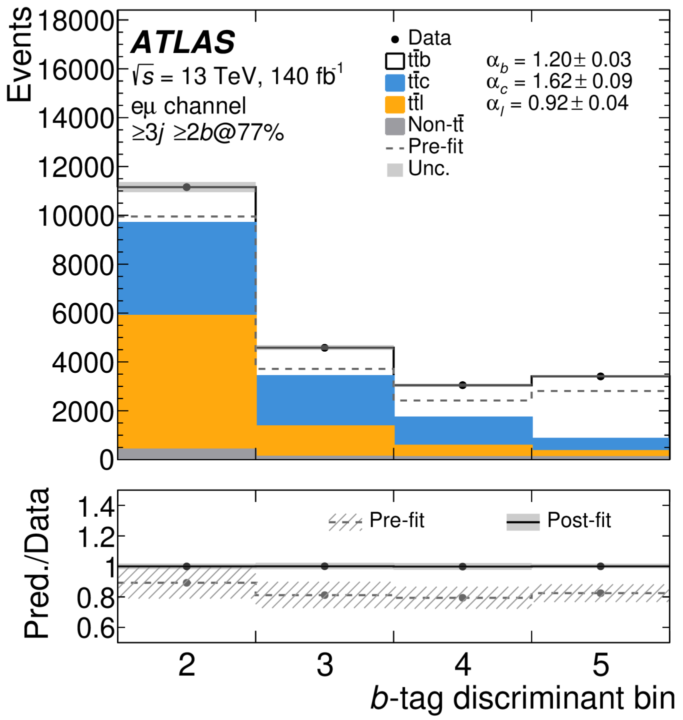

arXiv:2407.13473

$t\bar{t}+b$-jets production in $e\mu$ final state

	Inclusive region *Global* approach	Regions in terms of jet multiplicity and third-highest-p_T jet-p_T *Kinematic-dependent* approach	
	(nominal)	(systematic)	
Category	$\geq 3j \geq 2b$@77% ≥ 25 GeV	$3j \geq 2b$@77% 25–35 GeV | 35–50 GeV | ≥ 50 GeV	$\geq 4j \geq 2b$@77% 25–50 GeV | 50–75 GeV | ≥ 75 GeV
$t\bar{t}b$	$\geq$3 b-jets	$\geq$3 b-jets	–
$t\bar{t}b_{ex}$	–	–	exactly 3 b-jets
$t\bar{t}b\bar{b}$	–	–	$\geq$4 b-jets
$t\bar{t}c$	< 3 b-jets and ≥ 1 c-jet	< 3 b-jets and ≥ 1 c-jet	< 3 b-jets and ≥ 1 c-jet
$t\bar{t}l$	events that do not meet above criteria	events that do not meet above criteria	events that do not meet above criteria

Regions	Fitted values of scale factors α_b^s	α_{bex}^s	α_{bb}^s	α_c^s	α_l^s	Type
$\geq 3j \geq 2b$; ≥ 25 GeV	1.20 ± 0.03	–	–	1.62 ± 0.09	0.92 ± 0.04	*Global*
$3j \geq 2b$; (25–35) GeV	1.40 ± 0.15	–	–	1.99 ± 0.42	0.98 ± 0.08	*Kinematic-dependent*
$3j \geq 2b$; (35–50) GeV	1.30 ± 0.11	–	–	1.74 ± 0.27	0.77 ± 0.11	
$3j \geq 2b$; ≥ 50 GeV	1.26 ± 0.12	–	–	1.05 ± 0.27	1.09 ± 0.15	
$\geq 4j \geq 2b$; (25–50) GeV	–	1.31 ± 0.10	1.15 ± 0.14	1.93 ± 0.11	0.92 ± 0.01	
$\geq 4j \geq 2b$; (50–75) GeV	–	1.10 ± 0.09	1.20 ± 0.10	1.64 ± 0.09	0.86 ± 0.01	
$\geq 4j \geq 2b$; ≥ 75 GeV	–	1.10 ± 0.10	1.09 ± 0.10	1.25 ± 0.10	0.83 ± 0.02	

arXiv:2407.13473

$t\bar{t}$+ b-jets production in $e\mu$ final state

- An algorithm is developed for the classification of the origin of b-jets (from $t\bar{t}$ or gluon radiation).
- All possible permutations of b-jets, the one with the minimal $-\ln(w)$ is chosen, and the first two b-jets are assigned to top quarks

$$-\ln w = \begin{cases} \left(\Delta R_{\ell 1 b 1} - \Delta R^{\min}_{\ell 1 b}\right)^2 + \left(\Delta R_{\ell 2 b 2} - \Delta R^{\min}_{\ell 2 b}\right)^2 + \left(\max(\Delta R_{b1b3}, \Delta R_{b2b3}) - \Delta R^{\max}_{bb}\right)^2 & \text{if } N_{b\text{-jets}} = 3, \\ \left(\Delta R_{\ell 1 b 1} - \Delta R^{\min}_{\ell 1 b}\right)^2 + \left(\Delta R_{\ell 2 b 2} - \Delta R^{\min}_{\ell 2 b}\right)^2 + \left(\Delta R_{b3b4} - \Delta R^{\min}_{bb}\right)^2 & \text{if } N_{b\text{-jets}} \geq 4, \end{cases}$$

- **The algorithm correctly assigns 53% (56%) of b-jets in tt events with at least 3 (4) jets**
- **By selecting the leading pT b-jets, the fraction of correctly assigned b-jets is 42% (27%)**

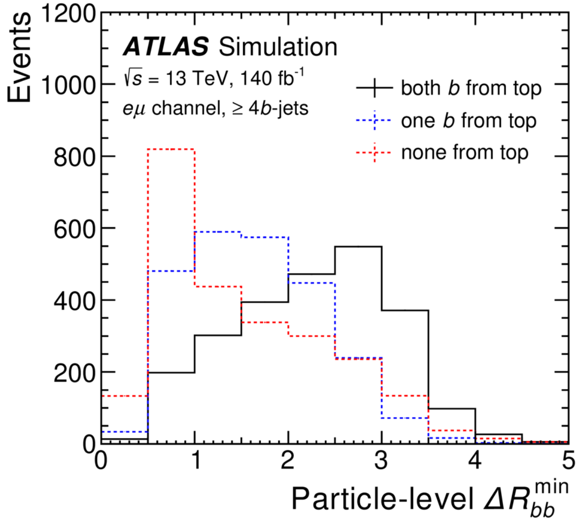

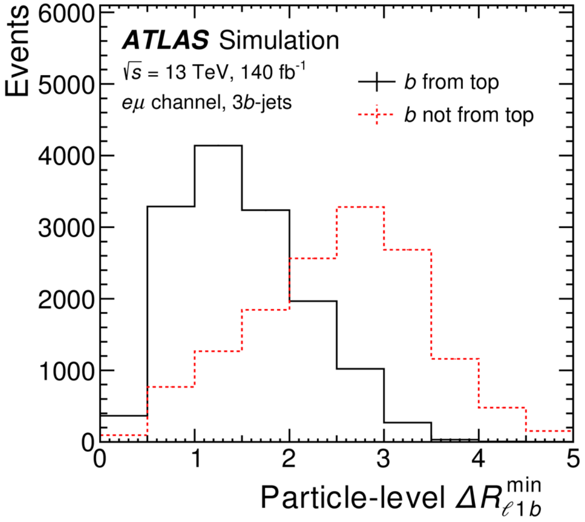

arXiv:2407.13473

$t\bar{t} + b$-jets production in $e\mu$ final state

- Unfolding

$$N^i_{\text{unfold}} = \frac{1}{f^i_{\text{eff}}} \sum_k \mathcal{M}^{-1}_{ik}\, f^k_{\text{accept}}\, f^k_{t\bar{t}b}\, (N^k_{\text{data}} - N^k_{\text{bkg}}),$$

$$f^i_{\text{eff}} = \frac{\mathcal{S}^i_{t\bar{t}b,\text{part}\wedge\text{reco}}}{\mathcal{S}^i_{t\bar{t}b,\text{part}}}, \qquad f^k_{\text{accept}} = \frac{\mathcal{S}^k_{t\bar{t}b,\text{reco}\wedge\text{part}}}{\mathcal{S}^k_{t\bar{t}b,\text{reco}}} \qquad f^k_{t\bar{t}b} = \frac{\mathcal{S}^k_{t\bar{t}b,\text{reco}}}{\mathcal{S}^k_{t\bar{t}b,\text{reco}} + \mathcal{B}^k_{t\bar{t}b,\text{reco}}},$$

$$\frac{1}{\sigma^{\text{fid}}} \cdot \frac{\text{d}\sigma^{\text{fid}}}{\text{d}X^i} = \frac{N^i_{\text{unfold}}}{\Delta X^i \sum_i N^i_{\text{unfold}}},$$

arXiv:2407.13473

$t\bar{t}+b$-jets production in $e\mu$ final state

- Fiducial cross-sections

Fiducial phase space	Fiducial cross-sections [fb] $\geq 3b$	$\geq 3b \geq 1l/c$	$\geq 4b$	$\geq 4b \geq 1l/c$
Measured	143 ±1 (stat) ±12 (syst)	87 ±1 (stat) ±8 (syst)	22 ±1 (stat) ±3 (syst)	14 ±1 (stat) ±2 (syst)
Powheg+Pythia 8 $t\bar{t}b\bar{b}$ (4FS)	132	78	23	14
Powheg+Pythia 8 $t\bar{t}b\bar{b}$ h_{bzd} (4FS)	129	74	21	13
Powheg+Pythia 8 $t\bar{t}b\bar{b}$ dipole (4FS)	128	71	22	13
Powheg+Pythia 8 $t\bar{t}b\bar{b}$ p_{T}^{hard} (4FS)	129	68	21	12
Powheg+Herwig 7 $t\bar{t}b\bar{b}$ (4FS)	130	77	22	14
Sherpa $t\bar{t}b\bar{b}$ (4FS)	135	90	21	15
Helac-NLO (off-shell) $e\mu + 4b$	–	–	20	–
Powheg+Pythia 8 $t\bar{t}$ (5FS)	120	74	18	11
Powheg+Herwig 7 $t\bar{t}$ (5FS)	128	75	18	11
MG5_aMC@NLO+Pythia8 $t\bar{t}$ (5FS)	122	72	18	11
MadGraph5_aMC@NLO+Herwig 7 $t\bar{t}$ (5FS)	110	66	13	8
Sherpa 2.2.12 $t\bar{t}$ (5FS)	124	73	16	10

arXiv:2407.13473

$t\bar{t}$+ b-jets production in $e\mu$ final state

- Fiducial cross-sections systematics

Source	Fiducial cross-section phase space			
	$\geq 3b$ Unc. [%]	$\geq 3b \geq 1l/c$ Unc. [%]	$\geq 4b$ Unc. [%]	$\geq 4b \geq 1l/c$ Unc. [%]
Data statistical uncertainty	1.0	1.2	3.9	4.8
Luminosity	0.8	0.8	0.8	0.8
Jet	3.4	5.2	6.6	8.5
b-tagging	5.1	4.9	6.5	6.4
Lepton and trigger	1.4	1.4	1.2	1.2
Pile-up	0.9	0.7	0.6	0.3
$t\bar{t}c/t\bar{t}l$ fit variation	1.7	1.7	0.8	0.8
$t\bar{t}c/t\bar{t}l$ shape variation	0.2	0.5	0.3	1.6
$t\bar{t}H/t\bar{t}V$ and non-$t\bar{t}$ background	1.1	1.1	2.2	2.4
Detector+background total syst.	6.7	7.6	9.7	11.2
Parton shower and hadronisation	2.9	3.5	1.5	3.6
μ_R and μ_F scale variations	0.7	0.6	0.2	0.3
Matrix element matching (p_T^{hard})	1.3	1.1	4.8	7.0
h_{damp}	1.8	1.5	2.9	3.2
ISR	0.1	0.4	0.2	0.3
FSR	3.1	3.6	3.3	3.1
RecoilToTop	1.8	1.9	2.4	3.4
PDF	0.2	0.2	0.1	0.1
NNLO reweighting	0.6	0.5	0.5	0.5
MC statistical uncertainty	0.2	0.2	0.5	0.6
$t\bar{t}$ modelling total syst.	5.2	5.7	7.2	9.7
Total syst.	8.5	9.6	12.1	14.8
Total	8.5	9.6	12.7	15.5

arXiv:2407.13473

$t\bar{t}$+ b-jets production in $e\mu$ final state

- Differential cross-section in 3j3b

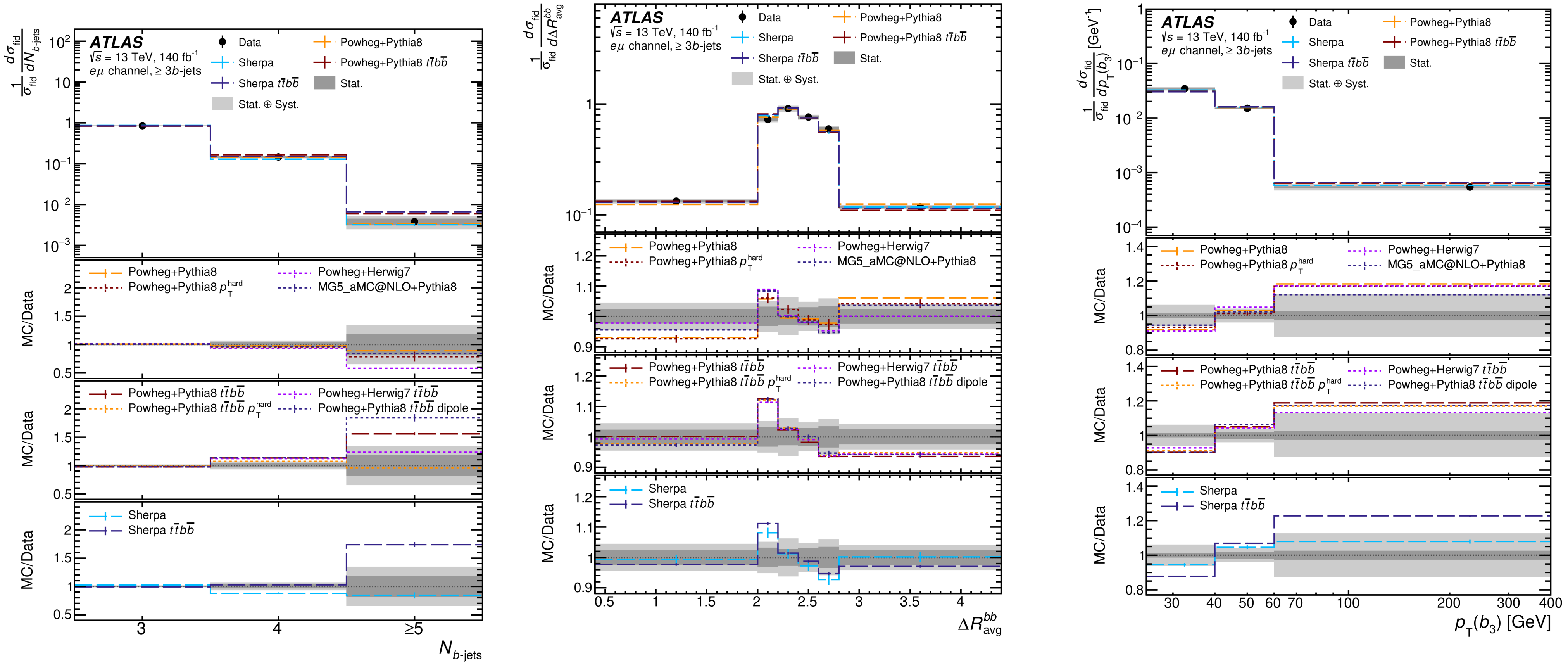

arXiv:2407.13473

$t\bar{t}+b$-jets production in $e\mu$ final state

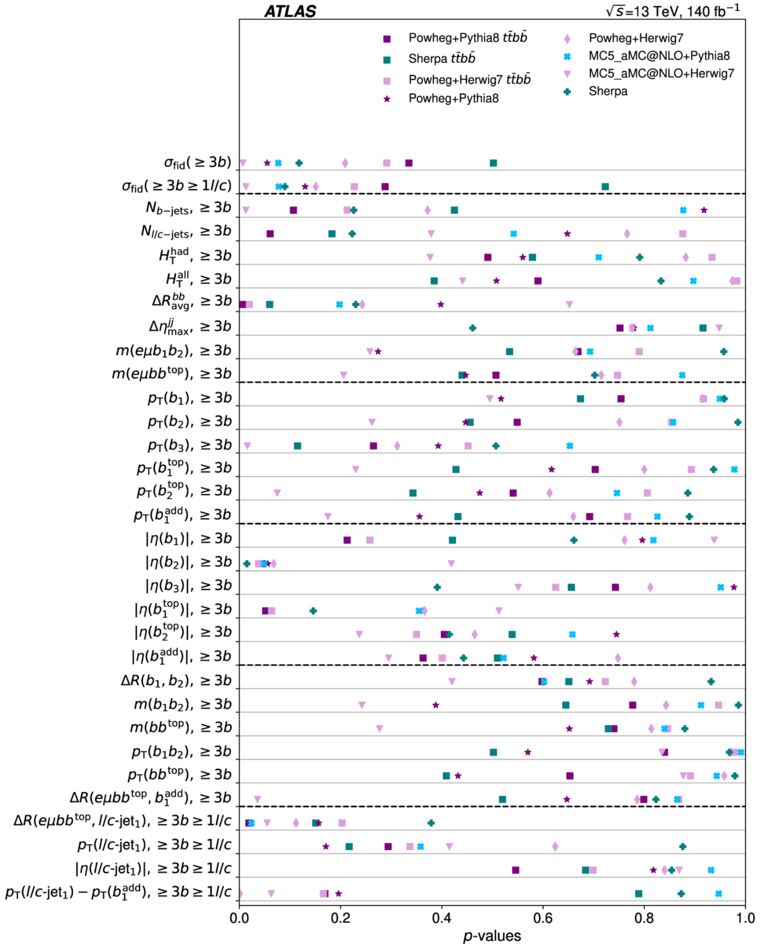

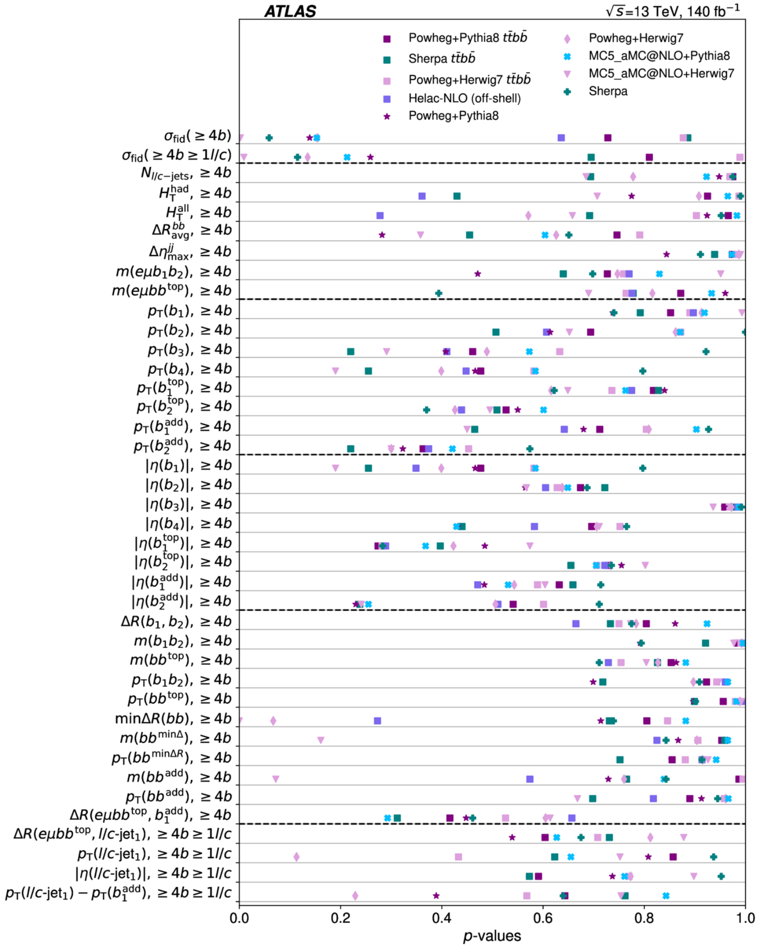

arXiv:2403.02133

LFU in W-boson decays to e, μ

- Pseudorapidity distribution of leptons in MC simulation with at least one b-jet

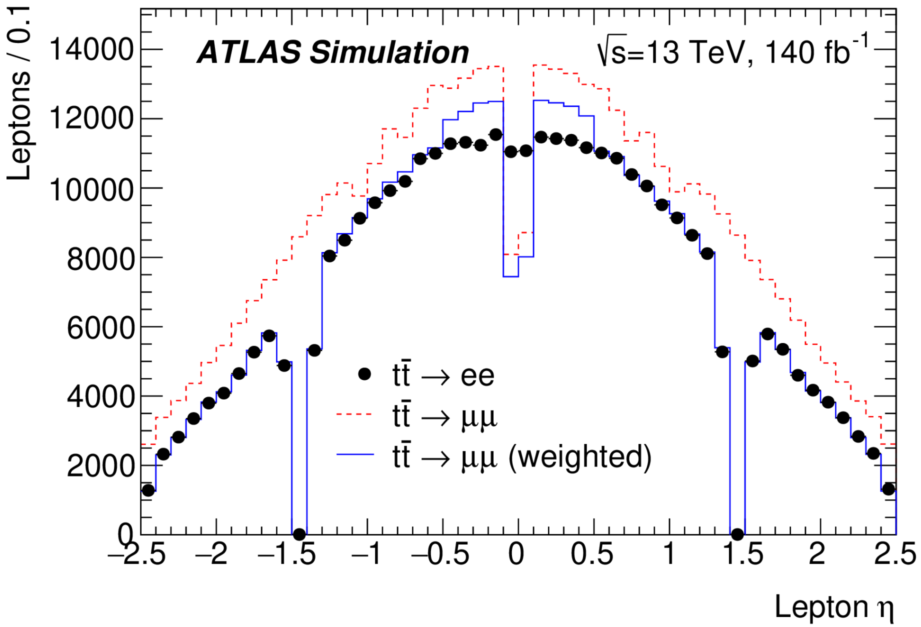

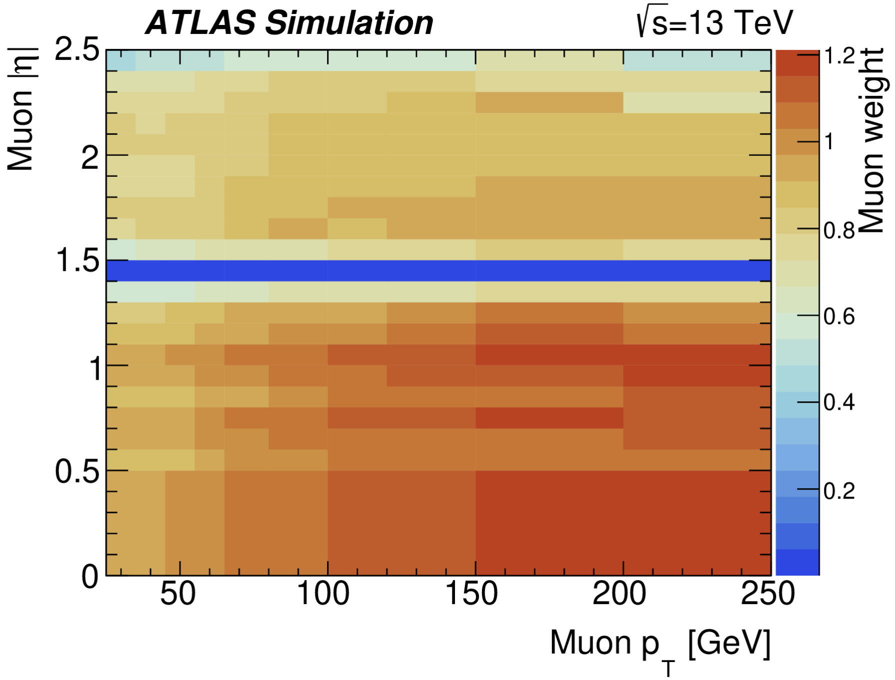

arXiv:2403.02133

LFU in W-boson decays to e, μ

- Object and event selection

Object selection		
Electrons	$p_T > 27.3$ GeV, $\lvert\eta\rvert < 1.37$ or $1.52 < \lvert\eta\rvert < 2.47$	
Muons	$p_T > 27.3$ GeV, $\lvert\eta\rvert < 2.5$	
b-tagged jets	$p_T > 30.0$ GeV, $\lvert\eta\rvert < 2.5$, b-tagging DL1r 70%	
Event selection	$t\bar{t} \to \ell\ell b\bar{b}\nu\bar{\nu}$	$Z \to \ell\ell$
Dilepton flavour ($\ell^+\ell^-$)	ee, $e\mu$, $\mu\mu$	ee, $\mu\mu$
Dilepton invariant mass	$m_{\ell\ell} > 30$ GeV	$66\text{ GeV} < m_{\ell\ell} < 116\text{ GeV}$
b-tagged jet multiplicity	1 or 2	–

arXiv:2403.02133

LFU in W-boson decays to e, μ

- Measurement of lepton isolation efficiencies – for $t\bar{t} \rightarrow ll$ events and compared to POWHEG+PYTHIA8 simulation samples

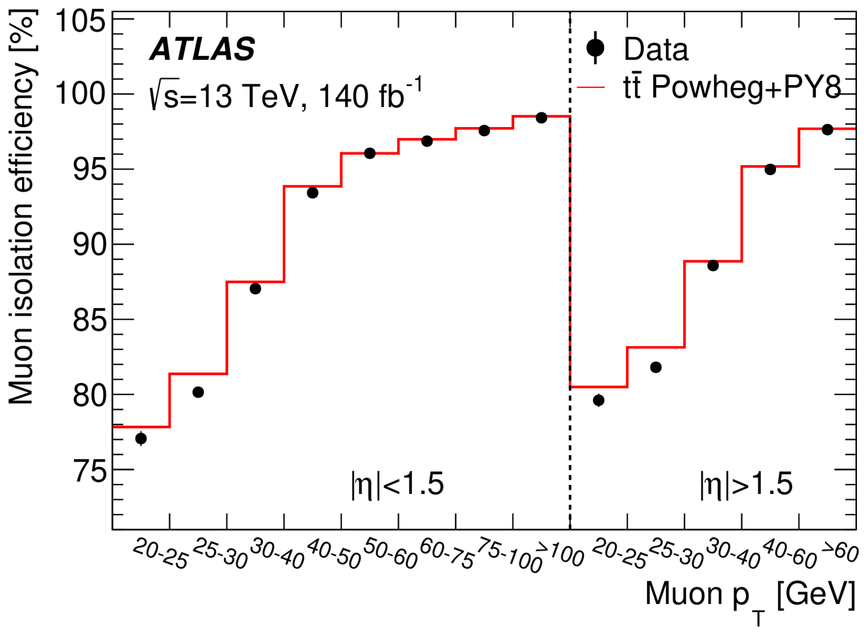

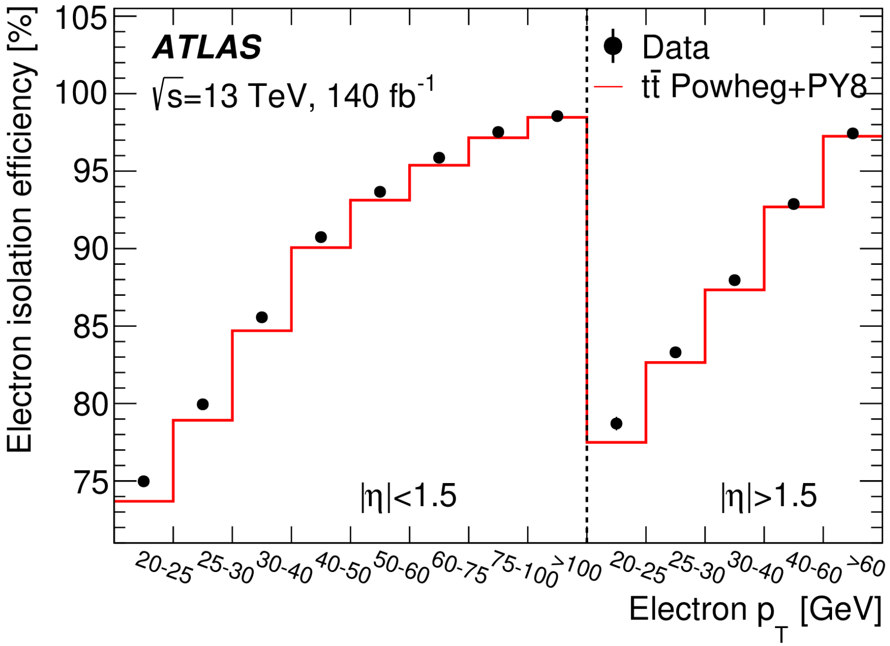

arXiv:2403.02133

LFU in W-boson decays to e, μ

- Measurement of lepton isolation efficiencies – for $Z \rightarrow ll$ events and compared to POWHEG+PYTHIA8 and SHERPA simulation samples

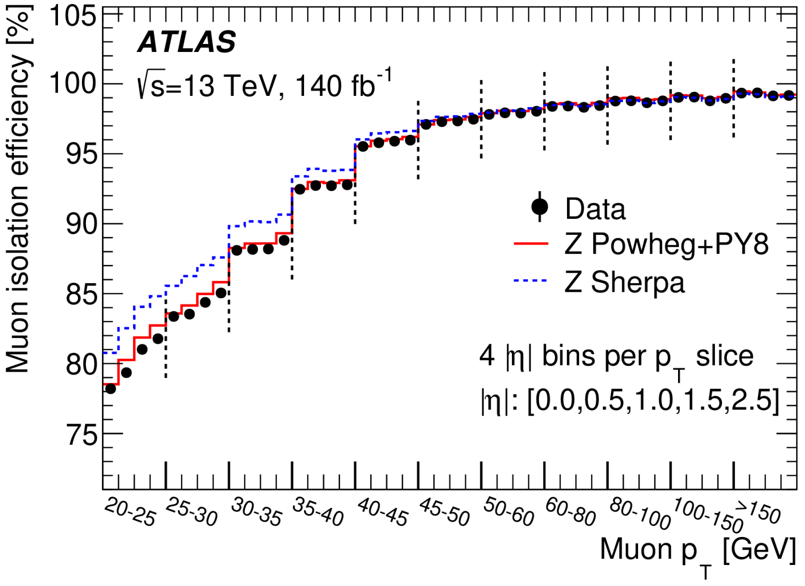

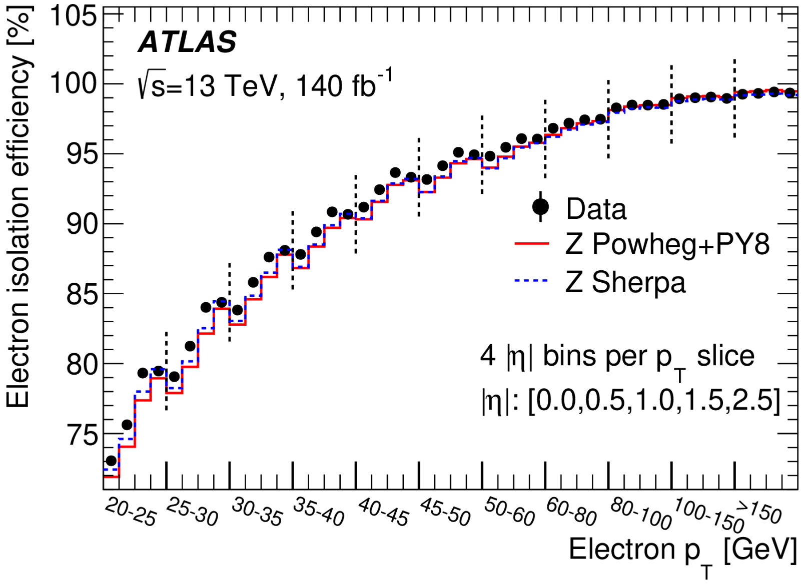

LFU in W-boson decays to e, μ

- The result for $R_{WZ}^{\mu/e}$ is changed by less that 0.01% when the first m_{ll} bin is removed from the fit
- Mismodelling in first bin consistent between ee and $\mu\mu$ (next slide)

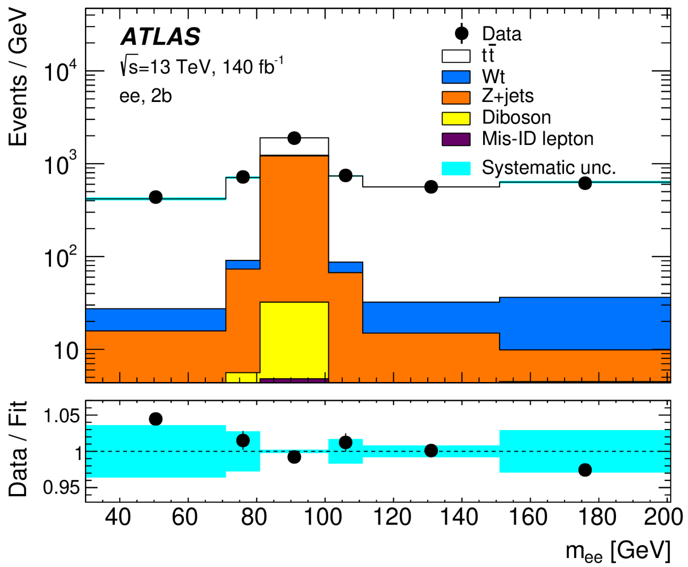

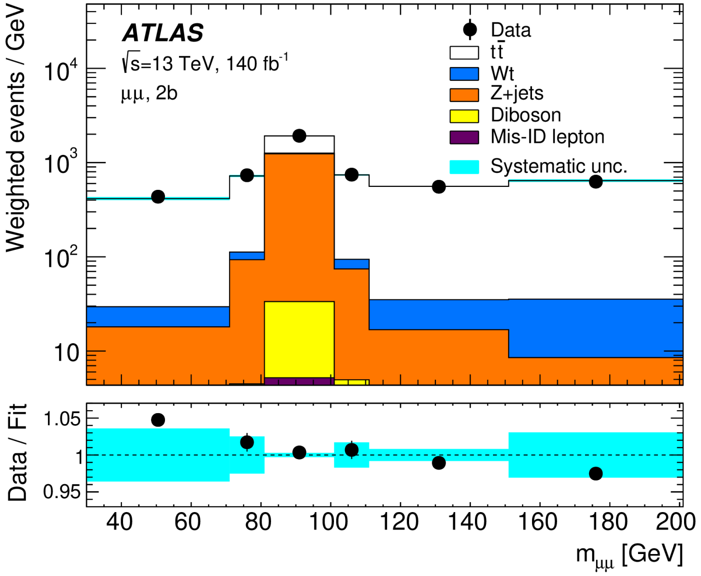

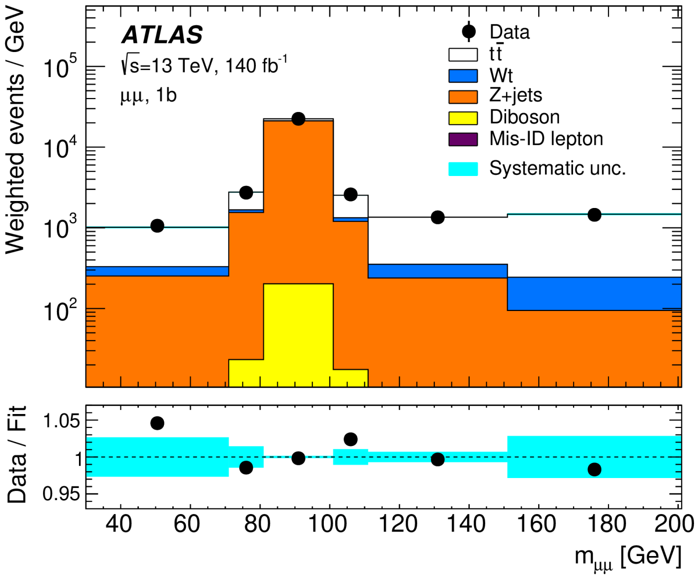

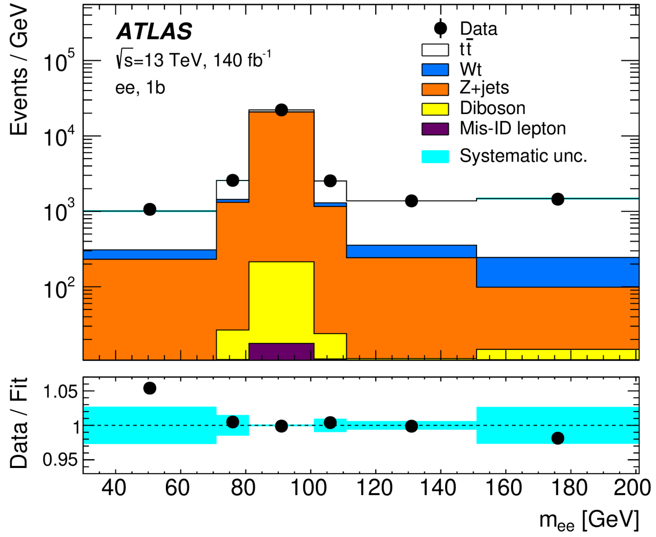

arXiv:2403.02133

LFU in W-boson decays to e, μ

- The result for $R_{WZ}^{\mu/e}$ is changed by less that 0.01% when the first m_{ll} bin is removed from the fit
- Mismodelling in first bin consistent between ee and $\mu\mu$
- Ratio of $\mu\mu$ over ee

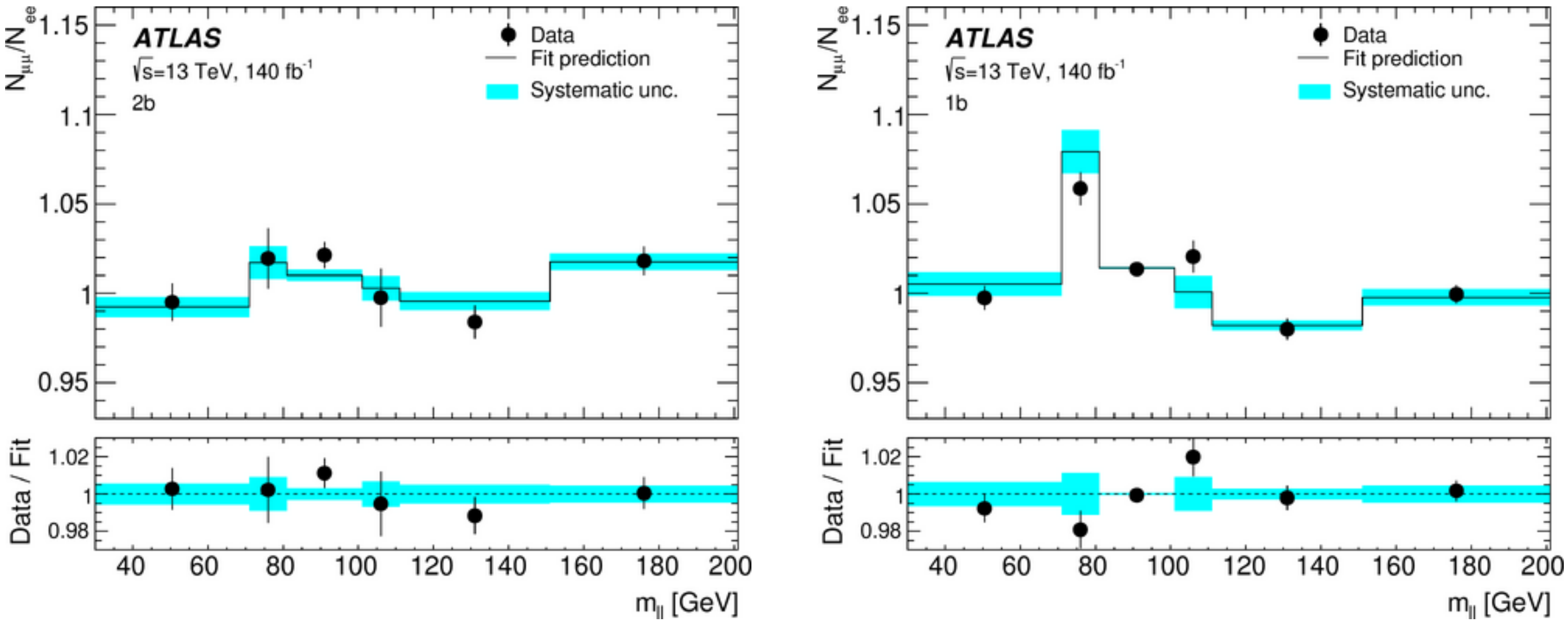

arXiv:2403.02133

LFU in W-boson decays to e, μ

- Statistical and systematic uncertainties

$$\sigma_{t\bar{t}} = 809.5 \pm 1.1 \pm 20.1 \pm 7.5 \pm 1.9\,\text{pb}\,,$$
$$\sigma_{Z\to\ell\ell} = 2019.4 \pm 0.2 \pm 20.7 \pm 16.8 \pm 1.8\,\text{pb}\,,$$

$$\sigma^{\text{fid}}_{Z\to\ell\ell} = 774.7 \pm 0.1 \pm 1.8 \pm 6.4 \pm 0.7\,\text{pb}\,.$$

- Uncertainties from data statistics, systematics, integrated luminosity, LHC beam energy, respectively.

Uncertainty [%]	$\sigma_{t\bar{t}}$	$\sigma_{Z\to\ell\ell}$	$R^{\mu/e}_{WZ}$	$R^{\mu\mu/ee}_{Z}$
Data statistics	0.13	0.01	0.22	0.02
$t\bar{t}$ modelling	1.68	0.03	0.10	0.00
Top-quark p_T modelling	1.42	0.00	0.06	0.00
Parton distribution functions	0.67	0.68	0.15	0.03
Single-top modelling	0.65	0.00	0.05	0.00
Single-top/$t\bar{t}$ interference	0.54	0.00	0.09	0.00
Z(+jets) modelling	0.06	0.73	0.13	0.20
Diboson modelling	0.05	0.04	0.01	0.00
Electron energy scale/resolution	0.05	0.06	0.10	0.11
Electron identification	0.10	0.07	0.04	0.13
Electron charge misidentification	0.06	0.06	0.01	0.13
Electron isolation	0.09	0.02	0.08	0.04
Muon momentum scale/resolution	0.04	0.02	0.06	0.04
Muon identification	0.18	0.12	0.11	0.23
Muon isolation	0.09	0.01	0.07	0.01
Lepton trigger	0.09	0.12	0.01	0.23
Jet energy scale/resolution	0.08	0.00	0.03	0.00
b-tagging efficiency/mistag	0.14	0.00	0.00	0.00
Misidentified leptons	0.17	0.02	0.15	0.05
Simulation statistics	0.04	0.00	0.06	0.00
Integrated luminosity	0.93	0.83	0.00	0.00
Beam energy	0.23	0.09	0.00	0.00
Total uncertainty	2.66	1.32	0.42	0.45

LFU in W-boson decays to e, μ

- Yields

Event counts	$N^{ee}_{1,\text{off}-Z}$	$N^{ee}_{1,\text{on}-Z}$	$N^{e\mu}_{1}$	$N^{\mu\mu}_{1,\text{off}-Z}$	$N^{\mu\mu}_{1,\text{on}-Z}$
Data	222304	442108	405437	223085	448105
$t\bar{t}$	154800 ± 1700	24830 ± 850	361000 ± 4200	152500 ± 1800	24070 ± 860
Wt	17500 ± 1600	2770 ± 240	41500 ± 3800	17800 ± 1700	2730 ± 250
Z+jets	46880 ± 400	410700 ± 2000	859 ± 21	51010 ± 780	418000 ± 2000
Diboson	770 ± 160	3940 ± 840	790 ± 280	770 ± 160	3880 ± 830
Mis-ID leptons	1300 ± 500	360 ± 260	1740 ± 610	390 ± 150	172 ± 87
Total prediction	221280 ± 550	442600 ± 1100	405900 ± 1800	222390 ± 670	448900 ± 1100

Event counts	$N^{ee}_{2,\text{off}-Z}$	$N^{ee}_{2,\text{on}-Z}$	$N^{e\mu}_{2}$	$N^{\mu\mu}_{2,\text{off}-Z}$	$N^{\mu\mu}_{2,\text{on}-Z}$
Data	85936	37704	198502	86169	38512
$t\bar{t}$	79750 ± 920	13340 ± 480	191000 ± 1800	79770 ± 830	13180 ± 450
Wt	2860 ± 760	400 ± 110	6700 ± 1600	2940 ± 740	423 ± 90
Z+jets	2675 ± 68	23610 ± 590	78 ± 2	3095 ± 87	24110 ± 600
Diboson	67 ± 23	550 ± 110	29 ± 8	71 ± 30	570 ± 110
Mis-ID leptons	400 ± 290	96 ± 59	720 ± 520	350 ± 160	104 ± 56
Total prediction	85760 ± 360	38000 ± 190	198510 ± 440	86230 ± 300	38380 ± 210

arXiv:2405.05078

$t\bar{t}$ production in p+Pb collisions

- Use top quarks to probe
  - nuclear PDFs (nPDFs) in kinematic region of Bjorken-$x \sim 5 \cdot 10^{-3} - 0.05$ and $Q^2 \sim m_t^2 \sim 3 \cdot 10^4$ GeV^2 - poorly constrained by other measurements in this kinematic region
  - gluon nPDF (**important for perturbative calculations in QCD**) which may increase the $t\bar{t}$ cross-section by 10% compared to pp collisions.

- Cross-section differences between the two isospin configurations (proton-proton and proton-neutron) are below 0.1%

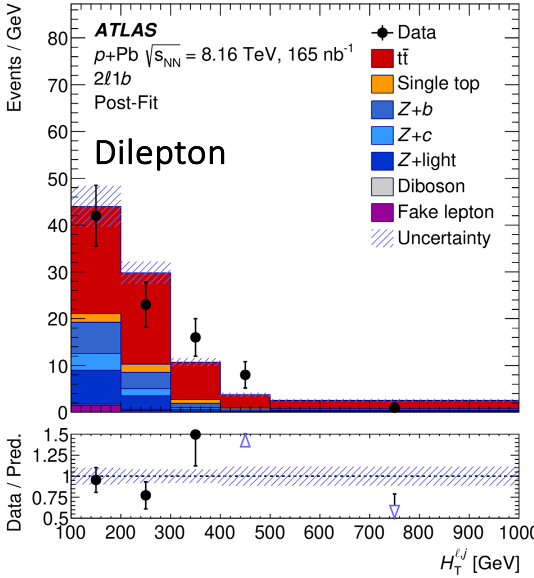

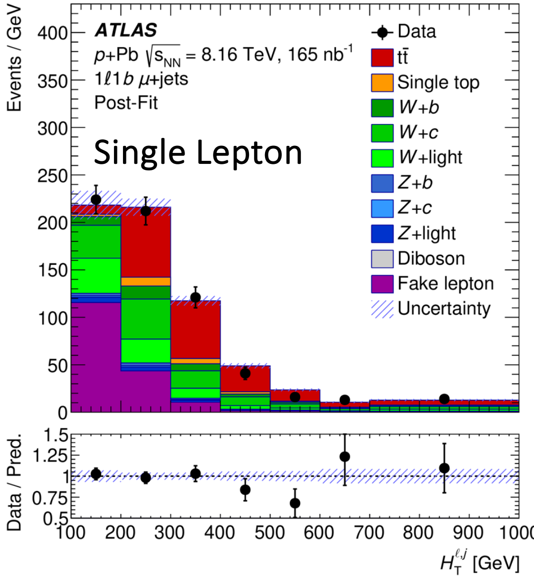

arXiv:2405.05078

$t\bar{t}$ production in p+Pb collisions

- Systematic uncertainties

Source	$\Delta\sigma_{t\bar{t}}/\sigma_{t\bar{t}}$ unc. up [%]	$\Delta\sigma_{t\bar{t}}/\sigma_{t\bar{t}}$ unc. down [%]
Jet energy scale	+4.6	-4.1
$t\bar{t}$ generator	+4.5	-4.0
Fake-lepton background	+3.1	-2.8
Background	+3.1	-2.6
Luminosity	+2.8	-2.5
Muon uncertainties	+2.3	-2.0
W+jets	+2.2	-2.0
b-tagging	+2.1	-1.9
Electron uncertainties	+1.8	-1.5
MC statistical uncertainties	+1.1	-1.0
Jet energy resolution	+0.4	-0.4
$t\bar{t}$ PDF	+0.1	-0.1
Systematic uncertainty	+8.3	-7.6

arXiv:2405.05078

$t\bar{t}$ production in p+Pb collisions

- Data and predicted post-fit yields in the SRs

	$1\ell 1b$ e+jets	$1\ell 1b$ μ+jets	$1\ell 2b$incl e+jets	$1\ell 2b$incl μ+jets	$2\ell 1b$	$2\ell 2b$incl
$t\bar{t}$	214 ± 24	194 ± 21	405 ± 21	373 ± 19	55 ± 6	79 ± 5
t-channel	6.9 ± 1.0	6.4 ± 1.0	7.7 ± 0.9	7.1 ± 0.9	0 ± 0	0 ± 0
W+b	37 ± 19	37 ± 19	16 ± 8	17 ± 9	–	–
W+c	120 ± 40	110 ± 40	14 ± 7	17 ± 8	–	–
W+light	80 ± 40	80 ± 40	4.8 ± 3.1	9 ± 5	–	–
Z+b	16 ± 13	8 ± 7	8 ± 7	3.7 ± 3.0	12 ± 9	2.9 ± 2.4
Z+c	9 ± 14	5 ± 7	1.7 ± 2.6	0.9 ± 1.4	6 ± 9	0.4 ± 0.6
Z+light	28 ± 16	12 ± 7	1.2 ± 1.1	0.9 ± 0.5	11 ± 6	0.34 ± 0.25
Diboson	0.32 ± 0.16	0.29 ± 0.15	0.055 ± 0.029	0.039 ± 0.02	0.53 ± 0.27	0.049 ± 0.025
tW	17.1 ± 3.0	15.5 ± 2.7	13.6 ± 3.2	12.1 ± 2.9	5.1 ± 2	2.4 ± 1.2
Fake lepton	630 ± 50	170 ± 40	110 ± 19	21 ± 12	1.9 ± 1	0.51 ± 0.27
Total	1154 ± 34	648 ± 24	582 ± 21	462 ± 18	91 ± 7	85 ± 5
Data	1162	641	570	464	90	97

arXiv:2405.05078

$t\bar{t}$ production in p+Pb collisions

- Measured $\mu_{t\bar{t}}$ value is translated to the inclusive $t\bar{t}$ cross-section via

$$\sigma_{t\bar{t}} = \mu_{t\bar{t}} \cdot A_{\text{Pb}} \cdot \sigma_{t\bar{t}}^{\text{th}},$$

- Where the mass number is $A_{Pb} = 208$ and $\sigma_{t\bar{t}}^{th}$ is the theoretical prediction of the $t\bar{t}$ cross-section in nucleon-nucleon collisions at NNLO precision (to normalise the signal $t\bar{t}$ samples in single lepton and dilepton decay modes)

arXiv:2405.05078

$t\bar{t}$ production in p+Pb collisions

- Dilepton post-fit

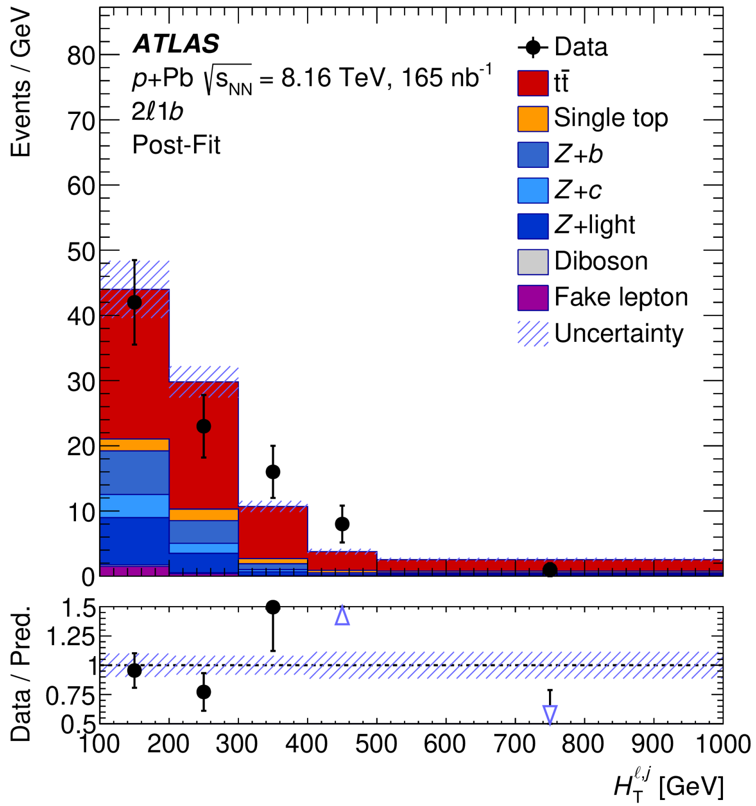

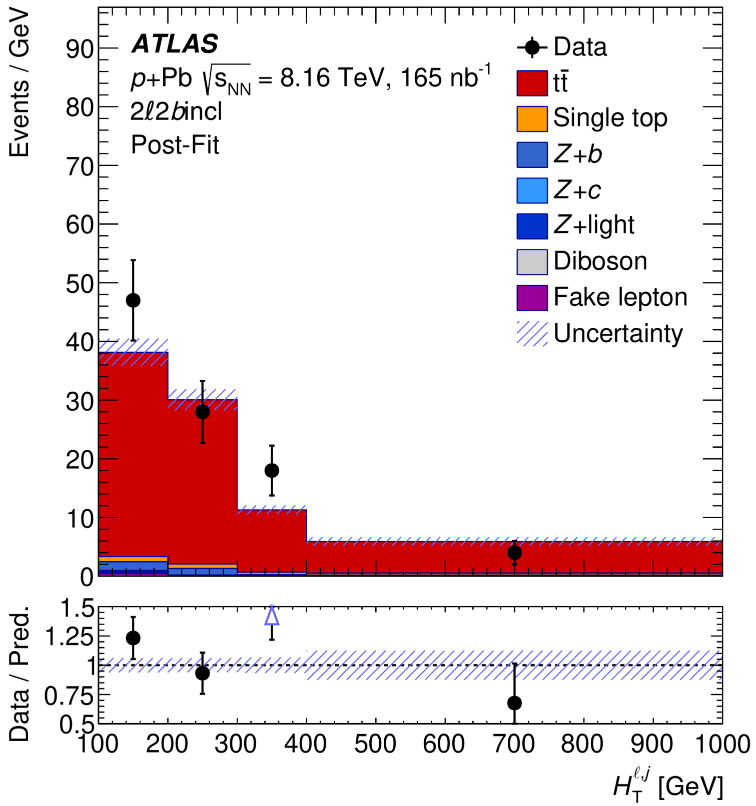

$t\bar{t}$ production in p+Pb collisions

- Lepton+jets post-fit

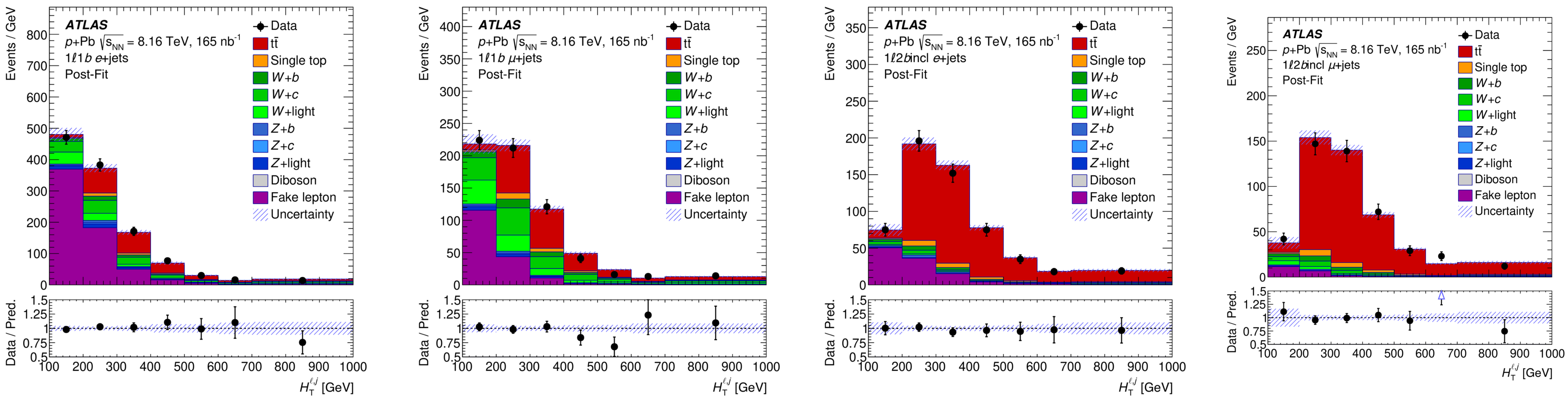

[arXiv:2405.05078](https://arxiv.org/abs/2405.05078)

$t\bar{t}$ production in p+Pb collisions

- The nNNPDF30 nPDF set shows the largest discrepancies
  - does not include the recent Run 2 LHC data for heavy-flavour production from p-Pb collisions